C, Sr and Cr isotope constraints on the depositional environment and palaeo-redox of the Neoarchean Fortescue Group, Pilbara Craton, WA

Thesis submitted in accordance with the requirements of the University of Adelaide for an Honours Degree in Geology/Geophysics

Liam Scarabotti

November 2019

THE UNIVERSITY of ADELAIDE

RUNNING TITLE:

Isotope constraints on depositional environment and redox of the Fortescue Group, WA

ABSTRACT

The Tumbiana and Hardey Formation of the Fortescue group in the Northern Pilbara Craton are Neoarchean sedimentary rocks dated at 2.7 Ga, with questionable palaeo-depositional environments ranging from possibly marine to continental lacustrine settings. In this study, we applied a set of traditional, novel isotopic (C, Sr and Cr) and trace element (REE, Zn/Fe) tracers, which were analysed in Neoarchean carbonates from recently recovered drill core 18ABAD01 intersecting the Tumbiana and Hardey Formations. This study generated high-resolution $\delta^{13}C$ and $^{87}Sr/^{86}Sr$ records, which provide convincing evidence for non-marine nature of these sediments, suggesting that these deposits were formed in a Neoarchean lacustrine system. Furthermore, this study applied palaeo-redox proxies such as $\delta^{53}Cr$ and Zn/Fe ratios, to infer past redox conditions during deposition of stromatolite-bearing carbonates from the Tumbiana Formation. Overall, results show these carbonates formed in a lacustrine settings and in presence of shallow oxic waters, the later likely produced due to local O_2 input from stromatolitic/ photosynthetic communities. Finally, results of this study have implications for the origin of local sediment-hosted stratiform copper SSC deposits. Importantly, the palaeo-redox data from Tumbiana Formation supports the existence of local pool oxic waters that could thus aid the formation of SSC deposits.

KEYWORDS

Depositional Environments, Palaeo-Redox, Fortescue Group, Pilbara Craton, Tumbiana Formation, Hardey Formation, Chromium Isotopes, Strontium Isotopes, REE

Contents

LIST OF FIGURES AND TABLES

INTRODUCTION

The Neoarchean (2.8 – 2.5 Ga) is a period dominated by single-cell life, this period predates the Great Oxygenation Event (GOE) in the Paleoproterozoic (2.4 – 2.2 Ga) (Gumsley et al., 2017), which changed life on the Earth by establishing a progressively more oxygenated ocean-atmosphere system (Sosa Torres, Saucedo-Vázquez, & Kroneck, 2015). The GOE thus led to changes in seawater redox, which in turn effected many chemical processes such as the emergency of banded iron formation and oxidative weathering (Johnson, Gerpheide, Lamb, & Fischer, 2014) resulting in changes to the Earth's biosphere and atmosphere (Hodgskiss, Crockford, Peng, Wing, & Horner, 2019). To investigate the state of the Earth's environments and marine redox before the GOE, this study looks to the Neoarchean sedimentary archives from a region in Western Australia in the Northern Pilbara Craton. Within part of the craton is the Fortescue Group, containing the Tumbiana and the Hardey Formation, see Figure 1. The Tumbiana Formation's paleo environment and local depositional settings are currently under contention, including the origin of a marine versus lacustrine setting for the formation of local Neoarchean microbial structures or stromatolites found in the region. Microbialites and stromatolites are remnants of photosynthetic life, specifically mats of microbes built by cyanobacteria over time becoming cemented into place and creating microbial or stromatolitic carbonates (Grey, 2009). As microbialites only form in shallow waters, presumably in the photic zone, there has been a debate in the literature over the lacustrine versus marine deposition of the Neoarchean Tumbiana Formation. The debate in the literature is founded on facies analysis and sedimentary structure analysis, with some articles finding a marine deposition (Packer, 1990; Thorne, 2001;

Coffey, Flannery, Walter, & George, 2013), while others finding a lacustrine environment (Bolhar & Van Kranendonk, 2007; R. Buick, 1992; Sakurai, Ito, Ueno, Kitajima, & Maruyama, 2005; Stanley & Buchheim, 2009). To weigh in on the debate, this study will use the 18ABAD01 drill core and selected geochemical and isotope analyses on sedimentary carbonates from the Neoarchean (~2.7 Ga) Tumbiana and Hardey Formation of the Fortescue Group. Specifically, C and Sr isotopes and trace elements are used to better constrain local depositional environments and further test the plausibility of marine versus lacustrine settings. For investigating the redox effects these oxygen producing cyanobacterial/stromatolitic communities would have had on the local environment, this study also analysed REE (Ce anomalies) and stable Cr isotopes δ^{53}Cr) which are considered sensitive palaeo-redox proxies.

When determining the Neoarchean palaeo-environments, one can use carbon isotopes (δ^{13}C) to verify a marine setting as Neoarchean marine δ^{13}C values range somewhere between -5 and 5 per mil (‰) when normalised against PDB (Shields & Veizer, 2002), and in contrast a presence of local methanogens should be recorded as more negative δ^{13}C values. For radiogenic Sr isotopes, the $^{87}Sr/^{86}Sr$ ratio in marine carbonate rock reflects a balance between Sr inputs from continental weathering (high $^{87}Sr/^{86}Sr$) versus hydrothermal sources (low $^{87}Sr/^{86}Sr$). This can be used to infer past palaeo-environments, specifically marine versus non-marine (lacustrine) settings, as the Neoarchean's expected marine or palaeo-seawater $^{87}Sr/^{86}Sr$ is approximately 0.702 - 0.703 (Kuznetsov, Semikhatov, & Gorokhov, 2018). Generally, if the Sr isotope composition of carbonates is more radiogenic (e.g. above 0.710 or higher) then this may instead indicate a lacustrine environment with granitic catchment, and alternatively if

the value is approximately 0.703 then this could indicate a lake setting in predominantly basaltic terrains (Kuznetsov et al., 2018).

To investigate palaeo-redox conditions at the time, we can look at redox sensitive metal isotopes and constrain whether there was any local or regional oxidation of shallow waters. The fractionation of stable chromium (Cr) isotopes occurs when the soluble Cr(VI) gets mobilised and partially reduced to Cr(III), which makes the chromium immobile and adsorb onto the surface of solid material (Li et al., 2016). As there was a potential change in redox conditions locally due to the stromatalitic life, and photosynthetic O_2 production, one can measure a change in $\delta^{53}Cr$ to see if heavy Cr isotope signals might correlate with local oxidation associated with stromatolite occurrences.

Examining the REE can further test such palaeo-redox scenarios via cerium anomaly (Ce/Ce*) tracers as Ce as a negative anomaly will occur under oxic marine conditions when cerium in sea water gets oxidised Ce(IV) will readily adsorb onto mineral surfaces, and thus become depleted in seawater, causing a negative Ce/Ce* anomaly (Tostevin et al., 2016).

Finally, the Zn/Fe ratios of carbonates can be used as a complementary palaeo-redox proxy. In anoxic waters both Zn and Fe are fairly soluable and thus enriched in seawater, but as water becomes more oxic iron is preferentially oxidised from soluble Fe(II) to insoluble Fe(III), but Zn is not affected as much, and thus oxygenation is expected to increase marine Zn/Fe ratios (Liu et al., 2015).

GEOLOGICAL SETTING/BACKGROUND

The Pilbara craton comprised partially of Archean highly deformed crust as well as weakly deformed late Archean sedimentary rocks lies in northwestern Western Australia. It can be divided into the East Pilbara Terrane (3.72 - 2.85 Ga), the Kuranna Terrane (3.3 – 3 Ga) and West Pilbara Terrane (~3.2 Ga) (Van Kranendonk, Hickman, Smithies, Nelson, & Pike, 2002). This study will look at the West Pilbara Terrane and at the specific formations that lie within, see Figure 2.

The West Pilbara Terrane is made up of the Karatha Terrane (3250 – 3270 Ma), the Regal Terrane (3190 Ma), the Nickol River Basin (3251 – 3269 Ma) and the Sholl Terrane (3118 – 3126 Ma) (Database, 1988).

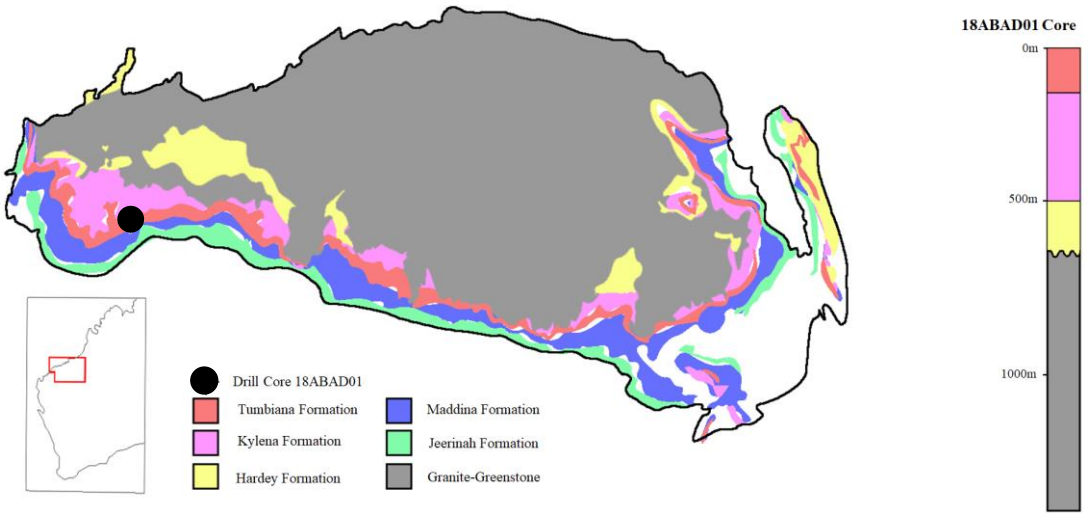

Figure 1: A broad overview of the Fortescue Group, showing the outcropping rock (Thorne, 2001) and the drill core 18ABAD01 provided by Artemis Resources Ltd. The white spaces are a combination of the Hamersley Group and younger rocks.

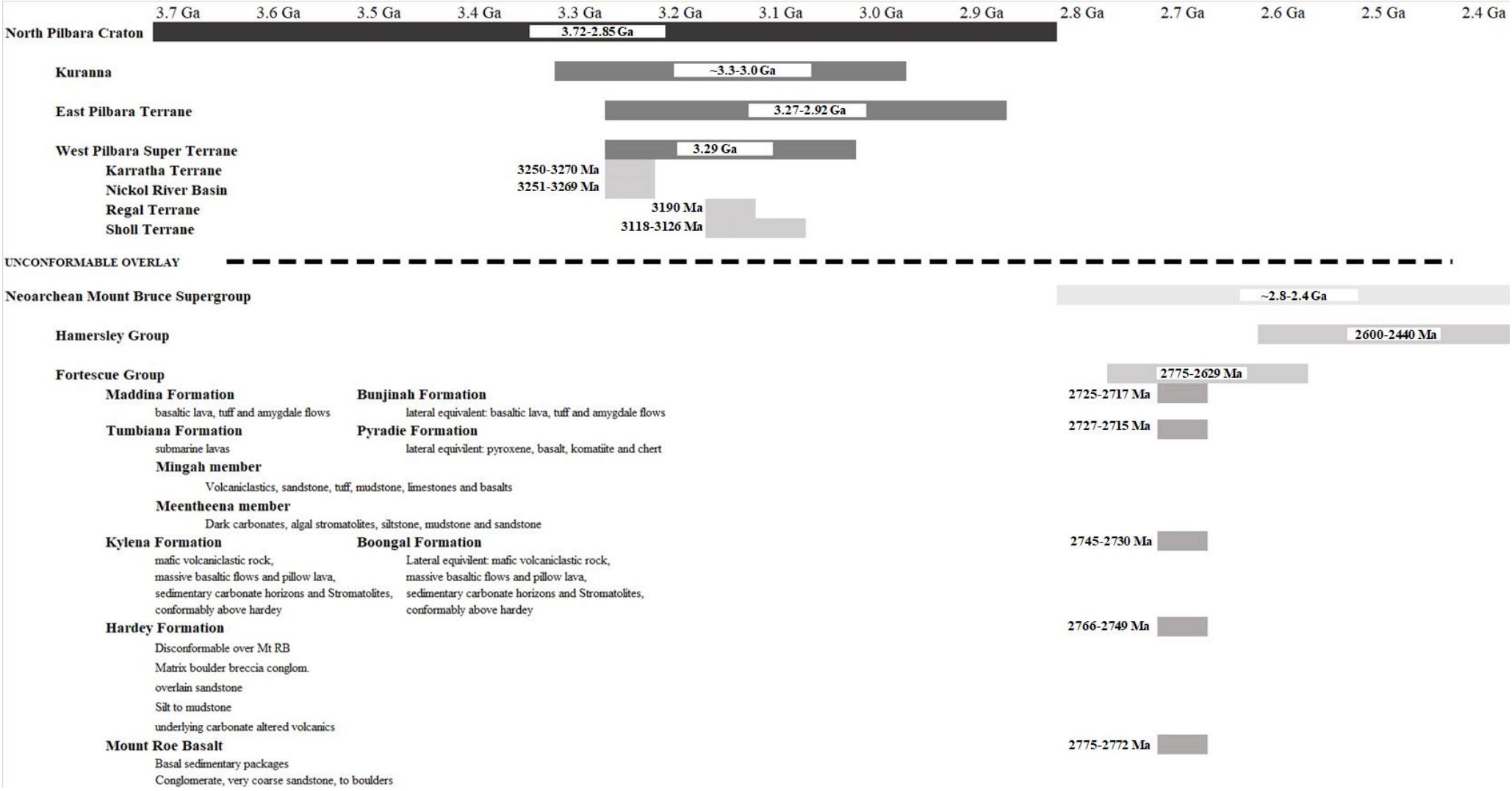

Figure 2: The time-space plot of the North Pilbara Craton its geological terranes, groups and formations including the Fortescue Group and its surrounding regions.

The focus of this study takes place in the Fortescue Group (2775 – 2629 Ma) unconformably overlaying the Sholl Terrane (3118 – 3126 Ma). The unconformity (2.8 - 2.4 Ga) is comprised of the Neoarchean Mount Bruce Supergroup, containing the Fortescue Group (2775 – 2629 Ma) (Van Kranendonk et al., 2002). The drill cores 18ABAD01 and 18ABAD02 drilled by Artemis Resources begin in the Tumbiana Formation and ends in a Granitic-greenstone basement unconformably overlain by the Hardey Formation.

Fortescue Group

A part of the Mount Bruce Supergroup, the 6.5km thick sedimentary and volcanic Fortescue Group is categorised into four stratigraphic units encompassing seven formations. The first comprises the Mount Roe Basalt and the Bellary Formation. The second contains the Hardey Formation. The third is the Boongal Formation, the Kylena Formation, the Tumbiana Formation, the Pyradie Formation and the Maddine Formation. The final unit contains the Jeerinah Formation (Thorne, 2001).

TUMBIANA FORMATION

The Tumbiana Formation is less than 200m thick and has a lateral equivalent conformably passing up into the Kylena Formation. The formation consists of stromatolitic rock with clastic carbonate, argillite, sandstone, primary and reworked tuff and minor conglomerate. The Tumbiana Formation is a lateral equivalent of the Pyradie Formation. The Pyradie Formation is up to 1.2km thick and is composed of pyroxene, spinifex-textured basalt flows, pillow lava, hyaloclastite, komatiite and minor chert

(Thorne, 2001). Typically the Tumbiana Formation is subdivided into two different members; the Mingah Member and the Meentheena Member. The Mingah Member is mainly volcaniclastics, sandstone, tuff, limestones, basalt and this member has the prevalence of stromatolites throughout (Stanley & Buchheim, 2009).

The Meentheena Member is characterised by dark carbonates, stromatolites, siltstone, sandstone and mudstone (Stanley & Buchheim, 2009).

The sub divisions of Tumbiana are loose and almost arbitrary due to multiple classifications being proposed to categorise the Tumbiana Formation but are commonly referred to by this classification (Sakurai et al., 2005).

KYLENA FORMATION

The Kylena Formation is 600m thick and both conformable and unconformable with the Hardey Formation and unconformably sits on the granite-greenstone basement. This formation is dominated by subaerial lavas, including subaqueous lavas and volcaniclastic rock. The Kylena Formation shares the lateral equivalent Boongal Formation, which conformably underlies the Pyradie Formation. The Boongal Formation is very similar to the Kylena Formation and includes more dominant subaqueous lavas and less subaerial lavas (Thorne, 2001).

HARDEY FORMATION

The Hardey Formation is a large formation, up to 3 km in thickness that disconformably overlies the Mt Roe Basalt, and comprises matrix boulder breccia conglomerate, overlain sandstone, silt to mudstone and underlying volcanics. The formation is thought to be part of four sections: the first being matrix boulder breccia conglomerate, the second being overlying conglomerate gravel, the third being sandstone overlying the second section and finally the top section being mudstone interbedded with sandstone (Thorne, 2001). The Hardey Formation also contains conglomerate-hosted gold mineralisation, however the paleo-placer is not well understood (Hall, 2005).

PREVIOUS WORK

Previous studies have looked at the Fortescue Group's component formations including U/Pb zircon dating (Hall, 2005), lithographic analysis (Sakurai et al., 2005) and some limited geochemical analysis (R Buick, 1992; Packer, 1990). The outcomes of the studies have varied, with some arguing a marine depositional setting and others a lacustrine setting. A previous study performing limited trace element analysis and carbon isotope analysis suggested a marine depositional environment (Coffey, Flannery, Walter, & George, 2013). This study and other geochemical studies however sourced samples from weathered outcrops which are suboptimal due to the alteration of rock chemistry during weathering processes. Another study analysing REE had contrasting

results to Coffey, Flannery, Walter & George, showing no change in Ce or Eu anomalies and suggested a lacustrine environment (Bolhar & Van Kranendonk, 2007).

METHODS

Sample Selection and Preparation

The analysis of strontium isotopes, and major and trace elements was based on a total of 73 carbonate rich rocks which were powdered by hardened steel ring mills at the CSIRO. These samples were focused on areas of interest outlined by carbon oxygen work and previous work conducted by the CSIRO.

The carbon and oxygen isotope analysis was carried out on 109 powdered samples using the same powdered rock. These samples were taken systematically from various depths to gain a broad understanding of the variability in isotopic composition and links to lithology, depositional environments and future areas of interest.

The analysis of chromium isotopes was performed on 15 samples which were cut and acid etched with ~1M HCl for 20 seconds to remove any areas in contact with metal that may have contaminated the rock. The samples were then milled using a tungsten carbide (WC) ring mill at University of Adelaide. These samples were selected from the Tumbiana Formation, with occurrences of stromatolites, to investigate possible palaeo-redox changes.

CARBON AND OXYGEN ISOTOPE ANALYSIS

Powdered carbonate rocks were weighed into a 5ml rounded bottom glass vial. The precise weight of the carbonate standards (NCM, UAC, ANU P3) that were run with samples were measured in small, medium and large quantities to match peaks between samples and standards, due to variable amounts of carbonate in studied bulk samples. The sample powders were sealed, its head space filled with helium gas removing any carbon gas, and then injected with seven drops of phosphoric acid dissolving the carbonate in the sample and turning it to carbon monoxide. The carbon monoxide gas was run through an IRMS to determine carbon and oxygen isotope ratios, the ratios found were standardised against the known standard of VPDB using the conventional delta notation, expressed as per mil (‰) variations:

$$\delta^{13}C = [(^{13}C/^{12}C)_{SAMPLE}/ (^{13}C/^{12}C)_{STANDARD} -1)]* 1000$$

and

$$\delta^{18}O = [(^{18}O/^{16}O)_{SAMPLE}/ (^{18}O/^{16}O)_{STANDARD} -1)]* 1000$$

STRONTIUM ISOTOPE ANALYSIS

The carbonate powders selected for Sr isotope analyses (i.e., $^{87}Sr/^{86}Sr$ ratios) were first leached with 3.6ml ultra-pure (20%) ammonium acetate (1M), in order to remove cations at exchangeable sites in clays, and to minimize detrital or clay-derived Sr contribution. This step was followed by adding another 3.6ml ultra-pure acetic acid, which takes carbonate into solution and excludes clays which can contaminate the strontium isotope data.

For each leaching the samples were (i) submerged in an ultrasonic bath for 30 minutes; (ii) centrifuged at 3600 rpm for 10 minutes; and (iii) for the final stage of leaching the supernatant was removed and collected for further analysis. The leached solutions in step one and two were removed and discarded, only the supernatant from step 3 was collected and placed in Teflon vials. At this stage, the centrifuge flasks were almost empty, but to recover most of the leached material, and the powders were rinsed twice with 1mL of DI water, centrifuged and that water was added again to the Teflon vials. An aliquot of each vial was taken for further analysis for Sr isotopes as well as trace and major elements. To purify Sr from a sample matrix, the leached samples were passed through Sr-specific columns following an established eluent chromatography method. Briefly, the dried down carbonate samples 1ml Nitric acid (8M) were added and passed through a Sr Micro Mio-Spin column specific resin which collects the Sr on the column and was washed with 8ml Nitric acid (0.05M). This was dried down and followed by an arbitrary ~0.5ml Nitric acid (15M) and ~0.25ml to oxidise any organics. Such purified Sr fractions were then dried down on a 140 degree hotplate and loaded into a rhenium filament using Brick's solution. These filaments were then analysed in the thermal

ionisation mass spectrometry (TIMS) using the Phoenix Isotopx instrument at The University of Adelaide.

RARE EARTH ELEMENT (REE), TRACE AND MAJOR ELEMENT ANALYSIS

An aliquot of sample from the final (3rd) leaching step (see above for details) was taken also for ICP-MS analysis of major and trace elements. The dried samples were diluted into a 100 times dilution using 2% HNO_3, and were further diluted into aliquots of 1000 and 10000 times dilution. The purpose of these dilutions was to analyse rare earth elements, trace elements and major elements. Whenever adding liquid to the samples or aliquots, measurements were taken to determine the final concentrations of selected elements. An additional set of multi-element standards were made up at concentrations of 0, 10, 20, 50, 100, 200 and 500 ppb as reference solutions for ICP-MS analyses. In addition, two carbonate standards JDo-1 and JLs were also analysed to validate the robustness and fidelity of measured element concentration data.

CHROMIUM ISOTOPE ANALYSIS

The analysis of stable chromium isotopes ($^{53}Cr/^{52}Cr$ ratios, or $\delta^{53}Cr$ values) of leached bulk carbonates was performed on 15 samples using the TIMS and double-spike approach. Briefly, the selected samples (rock chips or quarter cores) were cut and acid etched with ~1M HCl for 20 seconds to remove any areas in contact with possible metal that could have contaminated the rock. The samples were then milled using a tungsten carbide ring mill, and typically around ~500mg of sample was leached (dependent on chromium in sample) using 20mL of 0.5M HCl until there was no signs of effervescence. This was then centrifuged and the leachate placed in Teflon. The sample

solution was double spiked (4:1 ratio of sample to spike chromium ppm) with $^{50}Cr/^{54}Cr$ isotope tracer (i.e., double-spike) and dried down. After drying down the samples, 2mL of aquaregia was added to homogenise the chromium in spike and sample, and again dried down. The samples were then dissolved overnight in 20mL of DI water. Just before adding the samples to the column for eluent chromatography, the samples were: (i) sonicated for 1 hour; (ii) had 0.5mL of Ammonium Persulfate (APDS) added; (iii) set on a hot plate at 130 degrees Celsius until boiling and left for an hour to boil; and (iv) finally after boiling were set in a water bath to cool down. Below is a brief description of eluent chromatography (modified after Toledo, 2018) that was used for Cr separation from sample matrix:

The first column that was used was filled with a Bio-Rad AG 1-X8 100 – 200 mesh Anion resin, which was first washed with DI water, and then flushed with HCl that the resin was stored in. The resin was additionally cleaned with 5M HNO_3, 6M HCl and 0.1M HCl with DI water in-between cleans to rinse.

To the cleaned resin, each sample was loaded via pipette into a column and was flushed with 10mL followed by a 2mL wash of 0.2M HCl. The columns were then rinsed DI water.

Every step up until this point was put to waste, the waste beakers were then replaced with cleaned Teflon vials to collect the sample (i.e. Cr fraction) which was adsorbed to the resin. As the oxidiser slowly decomposed over time, there was a time constraint on how long the columns could work before the chromium began to drop out of the resin. This means that introducing the oxidiser to the sample required every step to be carried out with respect to time.

To collect the chromium (Cr) out of the resin, 1mL of 2M HNO_3 + 3 drops (5%) H_2O_2 was added to sit over the subsequent five minutes to oxidise the Cr. A further 5mL 2M HNO_3 + 7 drops (5%) H_2O_2 was added to flush out the Cr into the Teflon vial. Samples with pre-cleaned Cr fractions were then taken and dried down on a hotplate at 130 degrees Celsius.

The second column was necessary to remove any major amounts of iron (Fe) in the samples, as Fe is a major interference element for Cr (mass 54) which can thus cause isotope interferences and analytical problems on measured $\delta^{53}Cr$ values. To separate Fe, the same anion column was used again and anion resin was added ~2/3 ways up the column stem. To clean the resin 5M HNO_3 was added, followed by DI water to rinse. This was followed by adding 0.2M HCl, followed by 6M HCl. While the resin was cleaning, 1mL of 6M HCl was added to the samples which were then sonicated for two minutes to promote homogenisation and dissolution.

To the cleaned columns, the then dissolved samples with pre-cleaned Cr were added with its container placed underneath to catch the initial purified Cr coming through. To collect the remaining Cr from the resin, four repeating steps of 1mL of 6M HCl were added to each column. The samples with purified Cr were then again placed back on a hotplate at 130 degrees Celsius to dry down overnight.

The third column procedure was performed using Bio-Rad AG 50W-X8 200 – 400 mesh columns and cation resin, to get rid of any final impurities (e.g., alkali/alkaline metals) still present in pre-cleaned Cr fractions. For each column, 1/3 of the column stem was filled with the resin. The resin was then cleaned with DI water to rinse the acid storing the resin, followed by: 5M HNO_3 to clean, DI water to rinse off any remaining nitric acid, followed by 6M HCl to clean the resin, DI water to rinse out any

remaining HCl and a final rise with 0.5M HCl. To the dried down samples, i.e. the pre-cleaned Cr fraction, 100µL of 12M HCl was added and heated on a hotplate at 130 degrees Celsius for 10 minutes, and finished with 2.3mL of DI water to the samples which had been taken off heat.

The samples were then added to the columns with the same Teflon being placed under the column before it dripped through. To the collected samples, 8mL of 0.5M HCl was added and evaporated at 130 degrees Celsius.

Once the samples (i.e. final purified Cr fractions) were collected and dried down, they were then taken to the TIMS where prepared W filaments were loaded with an emitter of 1µL (2M) nitric acid and Nb_2O_5, and dried down at room temperature. The sample (Cr) was then loaded on the W filaments, by adding 2 µL of (2M) nitric acid to the samples and transferring it onto the filament. These were then dried down briefly at room temperature and further dried by passing ~5A current through the filaments to completely dry the sample, and remove any remaining organic components.

These filaments with purified and loaded Cr were then run on the TIMS Phoenix Isotopx instrument, using the double-spike approach. The collected and processed Cr isotope ratios ($^{53}Cr/^{52}Cr$) data, were used to calculate $\delta^{53}Cr$ values (in per mil) via normalisation to NIST 979 standard, based on the following equations:

$$\delta^{53}Cr = [(^{53}Cr/^{52}Cr)_{SAMPLE} / (^{53}Cr/^{52}Cr)_{STANDARD} -1)] * 1000$$

RESULTS

$\delta^{13}C$ isotopes analysis

For $\delta^{13}C$ isotope analysis, a total of 109 carbonate bearing rock samples were chosen to analyse. This was split into 50 for the Tumbiana formation and 59 for the Hardey Formation as seen in Figure 3. To maximise resolution, samples were taken at 0.1-5m intervals to detect any slight variations in the $\delta^{13}C$ record. The measured isotope values, normalised against VPDB, were all negative ranging from -8.6‰ to -3.08‰ in the Tumbiana and -11.76‰ to -2.43‰ in the Hardey. The samples were run on IRMS with an average error of the data at ±0.08‰ with four samples having errors of ±0.2-0.26‰. By the end of the analysis only 82 samples had data values due to low carbonate content throughout the rock of only a few percent w.t carbonate. This data was run three times to reduce errors in data and to reimage carbonate poor samples.

The Tumbiana carbonates tended to define a $\delta^{13}C$ trend from a lighter isotope signal to a heavier signal as the Tumbiana became older, the earliest samples from the Tumbiana were difficult to analyse due to limited amount of carbonate in these rocks.

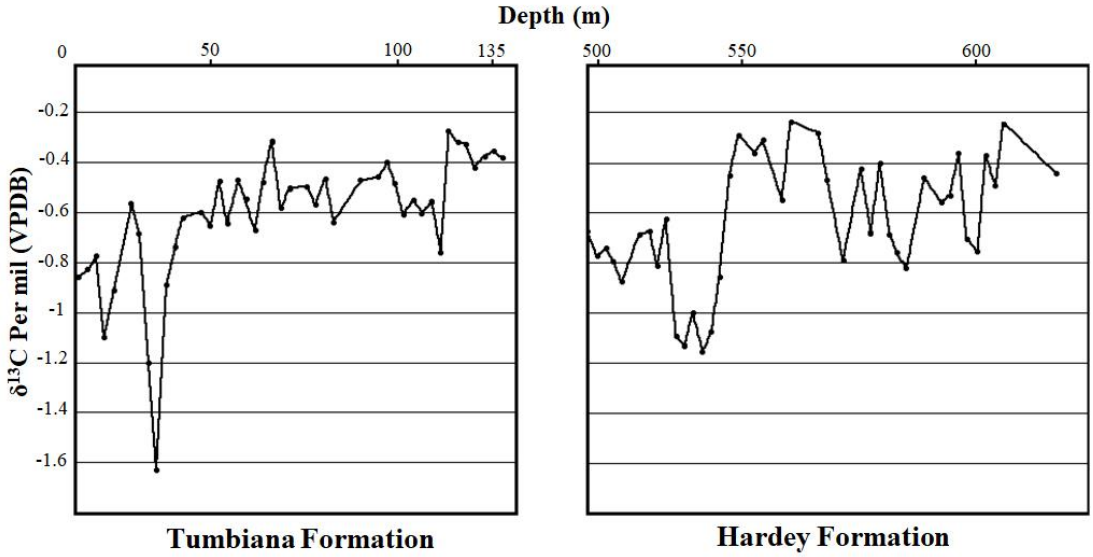

Figure 3: Stable carbon isotope ($\delta^{13}C$) values of the Tumbiana and Hardey Formation taken from 18ABAD01 drill core. The data is displayed as δ13C (normalised to VPDB) (per mil) vs depth (m).

The Hardey maintained a light carbon isotope compositions, with an anomalously light $\delta^{13}C$ peak of ~ -11‰, located between 530m to 561m, with a following transition to relatively heavier values of ~3.5‰.

$^{87}Sr/^{86}Sr$ Isotope Analysis

The analysed $^{87}Sr/^{86}Sr$ values are shown in Figure 4, a total of 77 samples were selected for Sr isotope analysis from 18ABAD01 drill core. This was focused mainly on the Tumbiana Formation with the aim to solve the depositional environment hypothesis (i.e. marine versus lacustrine) with samples taken at 0.1 - 5m intervals. The Hardey Formation had a lower resolution of sampling, where samples were taken at 5-10m intervals for the majority of the formation, but a higher resolution was focused around 530m-550m to further understand the anomalous negative spike in the $\delta^{13}C$ isotope data.

The samples were run on the TIMS and were further corrected for in-situ Rb-decay to correct for excess of in-situ generated radiogenic ^{87}Sr present in the bulk samples (Nurgalieva, Ponomarchuk, & Nourgaliev, 2007). Even after Rb correction, the $^{87}Sr/^{86}Sr$ results yielded quite radiogenic values ranging from 0.7209 to an anomalous peak of 1.1666. The Tumbiana Formation generally trends from a low 0.7209 values toward a more radiogenic values around 80-100 m reaching 0.77598, and two additional highly radiogenic values of ~0.900 and ~0.860 have been also detected at depths of 69 m and 90 m respectively. The $^{87}Sr/^{86}Sr$ trend then becomes lower as Tumbiana gets older reaching values around ~0.730. The Hardey Formation has general $^{87}Sr/^{86}Sr$ values of about 0.725, there is a radiogenic anomaly around 550 m and 573 m with a peak of 0.781 and a smaller peak at 605 m of 0.758.

This observed $^{87}Sr/^{86}Sr$ trend in the Tumbiana matches up with lithology where the generally more radiogenic samples are associated also with the presence of stromatolites suggesting locally restricted lacustrine settings. The $^{87}Sr/^{86}Sr$ trends in the Hardey Formation correlate with the peak associated with a negative $\delta^{13}C$ values in this formation. Also, the purported methanogenic and extremely negative $\delta^{13}C$ peak in the Hardey Formation (from 530m to 561m), seems to correlate with a slight dip in $^{87}Sr/^{86}Sr$ data.

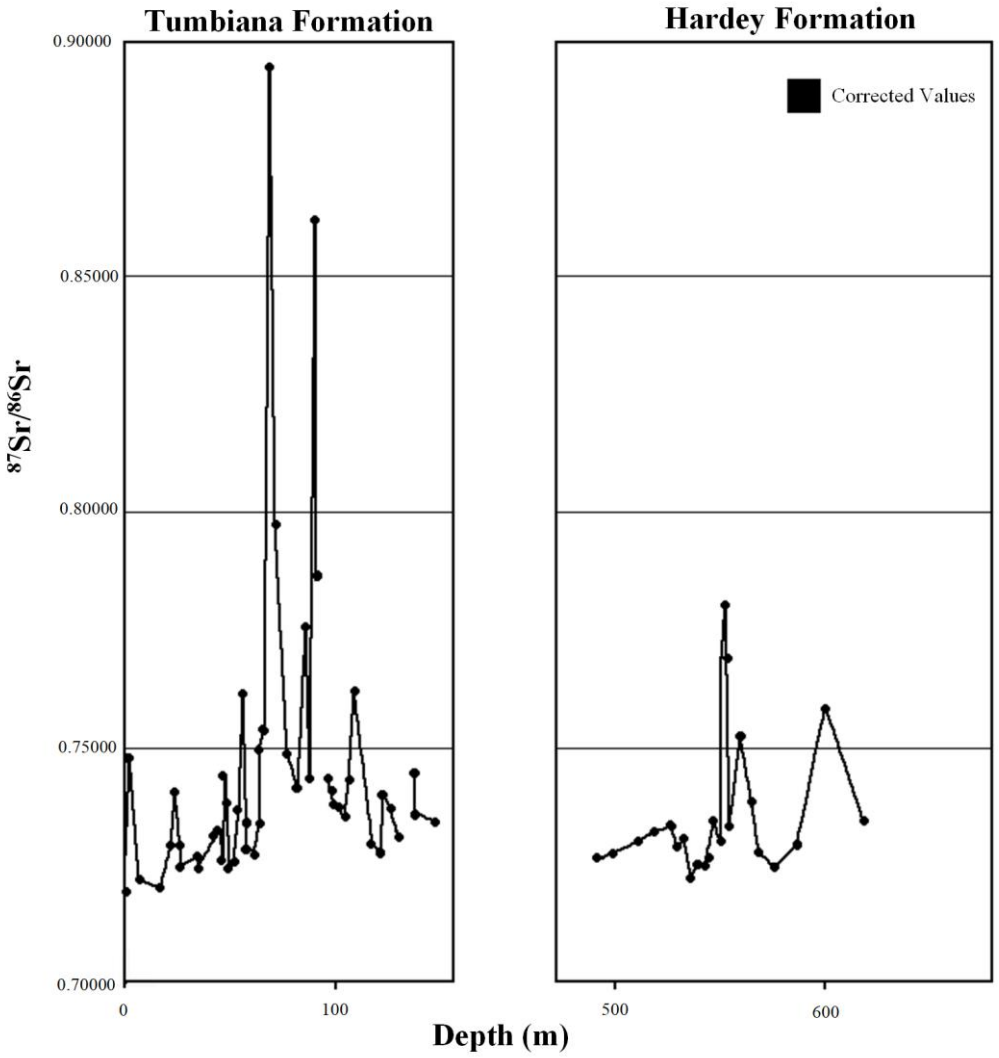

Figure 4: The combination $^{87}Sr/^{86}Sr$ isotope data of carbonates from the Tumbiana and Hardey Formations. All values have been corrected for in-situ Rb decay. Note that two outlier and vey radiogenic data points are not shown as they would plot out of scale.

Rare Earth Elements, Trace and Major Element Analysis

The full set of ICP data was selected from aliquots of the 77 Sr samples. This gave an exact resolution and focus area for future TIMS Sr work. The data included the full suite of REE (except for Pm), trace and major elements spread out over 1000 and 10000 times dilutions. The full set of REE was analysed for distinct patterns in the variations

of the Light REE (LREE), Middle REE (MREE) and Heavy REE (HREE). The REE suite of the Tumbiana Formation was noisy as seen in Figure 5.

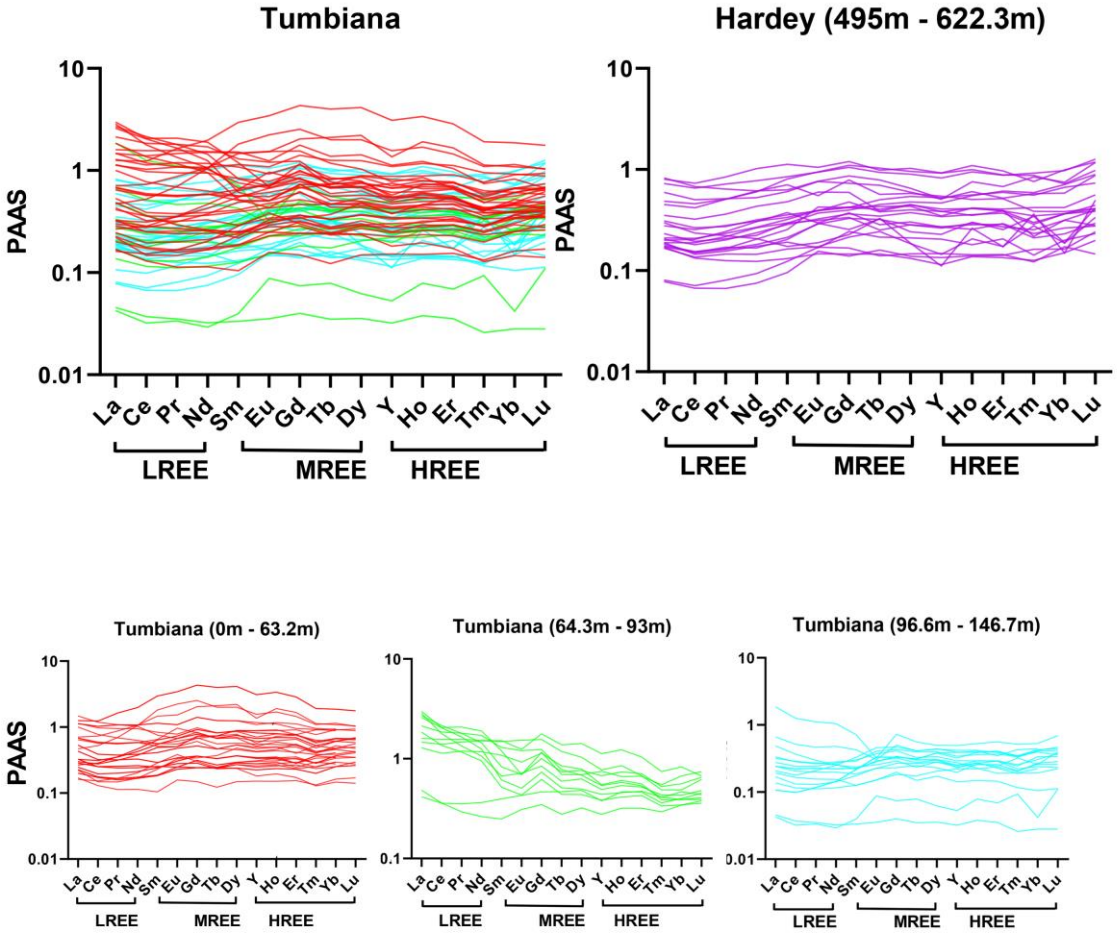

Figure 5: The spider plot over the two formations. The Tumbiana Formation has been split into three distinct areas: the start (0m to 63.2m), the middle (64.3m to 93m) and end (96.6m to 146.7m). The Hardey Formation with less data points has been kept as one, the REE have been divided into their heavy, medium and light components.

This was resolved by separating out the formation into three distinct segments that, according to Sr data, indicates a different environment. Following this data, a set of REE were analysed for any anomalies as seen in Figure 6.

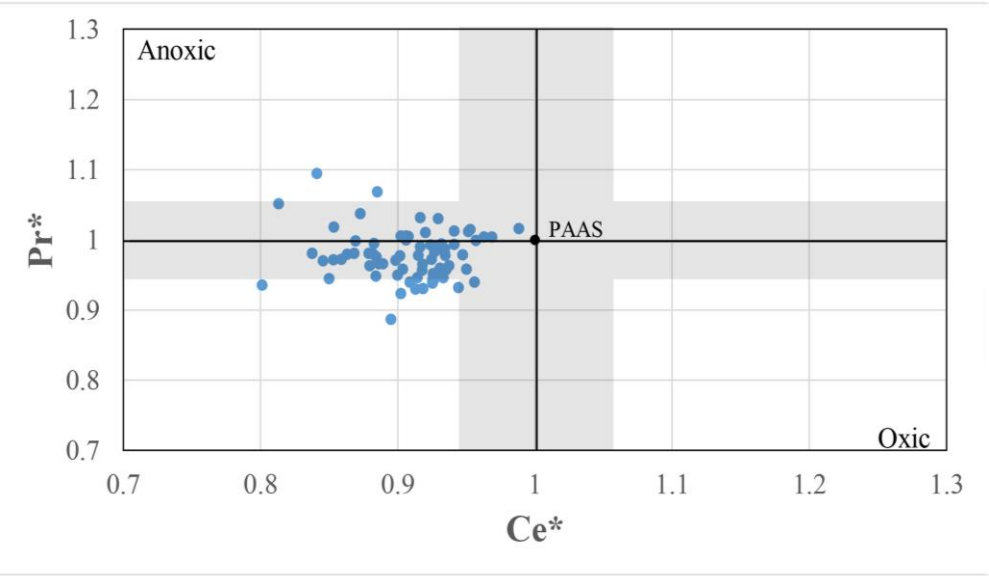

Figure 6: Figure of the Ce* anomaly. The Ce* vs Pr* where the signal is mainly in the undetermined region of error.

The first analysed REE was looking at Cerium anomalies which showed values ranging from 0.8 and 1 and showed horizontal trending data. The second anomaly investigated was Europium, which showed values ranging from 0.5 to 1.5 and the data trended horizontally. Finally, the ratio Zn/Fe was investigated and converted into a mol*10^4 ratio, see Figure 15.

The final data showed a peak in the Tumbiana Formation at 189.7 and trended in a parabolic peak over ~80 - 140m, the data in the Hardey Formation showed a flat trend in data, this peak corresponds with range of restriction that is purveyed in the $^{87}Sr/^{86}Sr$ ratios. The error in the ICP analysis was ~5- 10% error and was corrected for instrumental drift using known laboratory standards.

δ^{53}Cr Isotope Analysis

The Chromium isotope analysis was initially undertaken on a pool of 81 samples but was focused on 13 samples to image potential areas of redox. These samples were focused solely on the Tumbiana Formation with an emphasis over the 70 - 140m range. Of the 13 samples, 10 were successfully run due to the variable nature of the chromium analysis. As seen in Figure 7, the data peaks at δ^{53}Cr 0.41 and the majority of data is clustered between -0.2 and 0.2, these samples were corrected by 0.83 which was measured by 979 NIST samples to correct for the TIMS machine bias. The error of each sample is 0.12 to two standard errors, with the concentrations of chromium in each sample varying from ~20 to 75 ppm. These concentrations vary from values attained from the ICP-MS due to interference elements skewing data in the ICP, the concentrations measured in the TIMS are more reliable. Two data points were not included due to their high error. The high error rate is most likely due to either under spiking or variations in loading the sample.

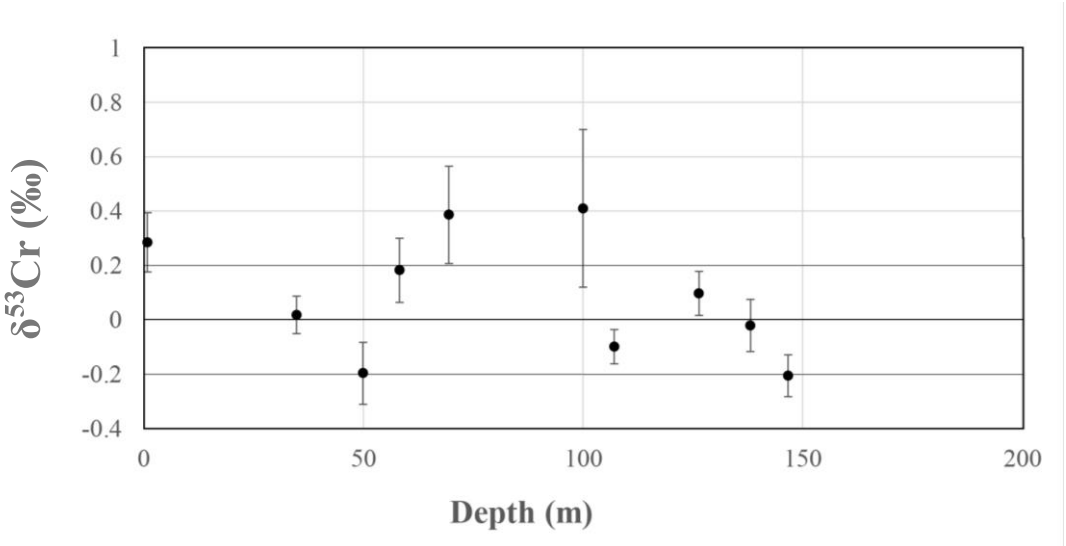

Figure 7: The δ^{53}Cr curve is of the Tumbiana Formation through the drill core, the values are plotted in δ^{53}Cr (‰) vs depth (m).

DISCUSSION

Assessment of Diagenesis and Detrital Contamination

CHANGES OF ELEMENTAL AND ISOTOPE COMPOSITION OF CARBONATE DUE TO METEORIC DIAGENESIS – FLUID/ROCK INTERACTIONS

To reliably interpret Sr isotopic and trace element data from sedimentary carbonates in terms of palae-environments, one needs to carefully check and evaluate potential detrital /clay contamination and also the effects of meteoric diagenesis.

Typically diagenetic effects cannot be determined with certainty through just one method, as the processes which alter and reset a carbonate rock vary with factors of pressure, temperature, chemical composition, water interactions, etc (Swart 2015). However one can test for specific factors that could have caused diagenesis in order to rule out potential problematic samples that have been altered. As an added benefit this method also shows samples least altered via these secondary processes, which in turn allow us to identify the best preserved, or least altered samples, and thus primary isotope signatures.

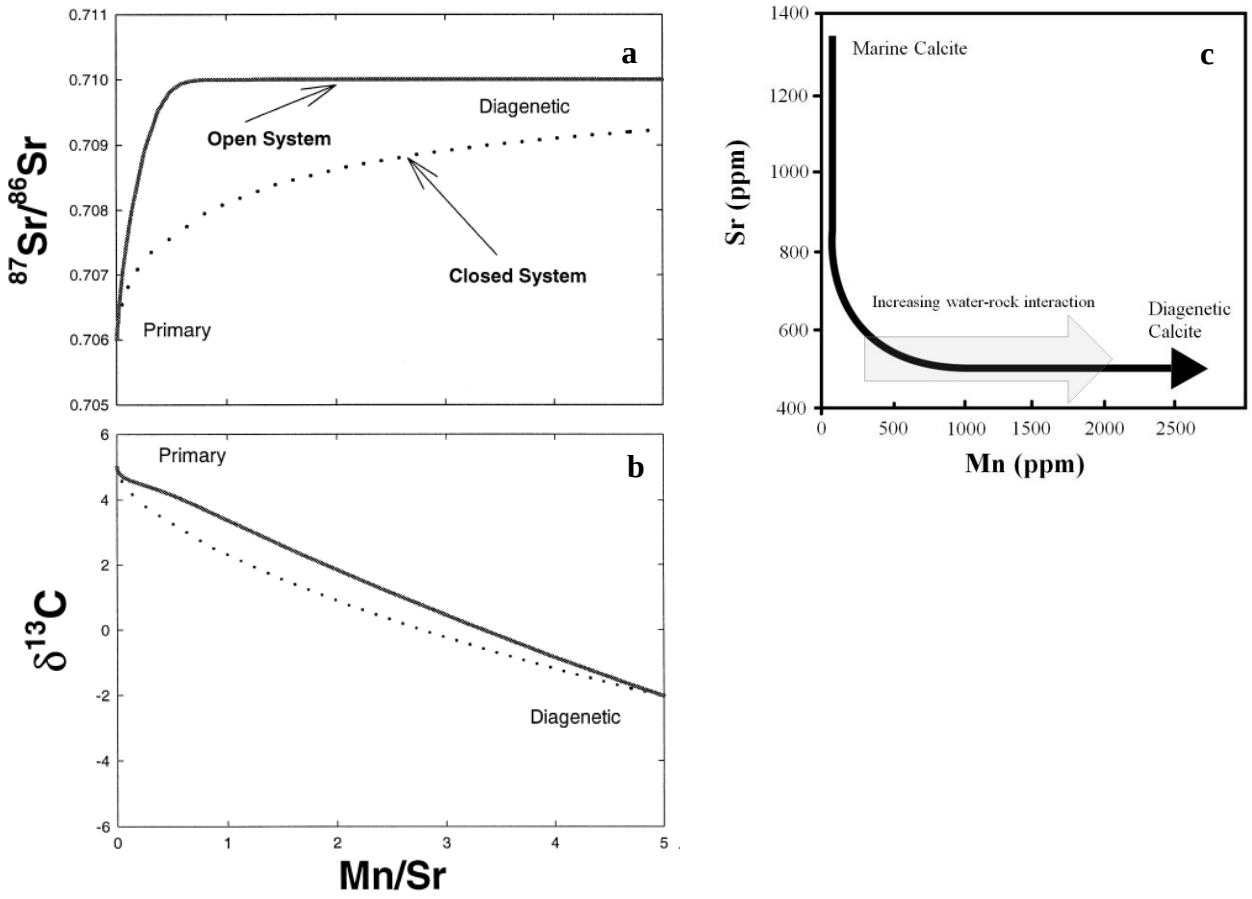

Figure 8: (c) Diagenetic trend showing that increase of diagenesis causes lower Sr and higher Mn concentrations in altered marine carbonates (modified from Banner & Hanson, 1990). (a, b) The effects of diagenesis on both $^{87}Sr/^{86}Sr$ and $\delta^{13}C$ values in marine carbonates in and open versus closed system (modified from Jacobsen et al., 1999).

Progressive alteration of marine carbonates via diagenesis would thus generate signals that would not reflect primary isotope signature during carbonate deposition. These diagenetic processes thus reset Sr and C isotopic ratio which can reflect signals that are very different to the original $^{87}Sr/^{86}Sr$ and $\delta^{13}C$ values. Typically, a comparison or cross-plot $\delta^{13}C$ and $\delta^{18}O$ data can be used to test for mixing of diagenetic carbonates and primary carbonate signals, where a statistical correlation indicates evidence of diagenesis (Banner & Hanson, 1990).

An elemental check for diagenesis can be done by observing the concentration of Mn throughout the samples, or Sr/Mn ratios, and comparing them against $^{87}Sr/^{86}Sr$. As Mn was observed to preferentially replace Sr as fluid rock interaction increases, a decrease in Sr/Mn ratio is observed along with changes in Sr and C isotopes, see Figure 9 (Banner & Hanson, 1990). Based on the later study and expected diagenetic trends, one can observe if diagenetic fluid alteration is present and detectable in our samples (see, Figure 9). One can also look at a $\delta^{13}C$ vs Mn/Sr trend to observe if there has been any meteoric diagenesis trackable in the carbon isotopes.

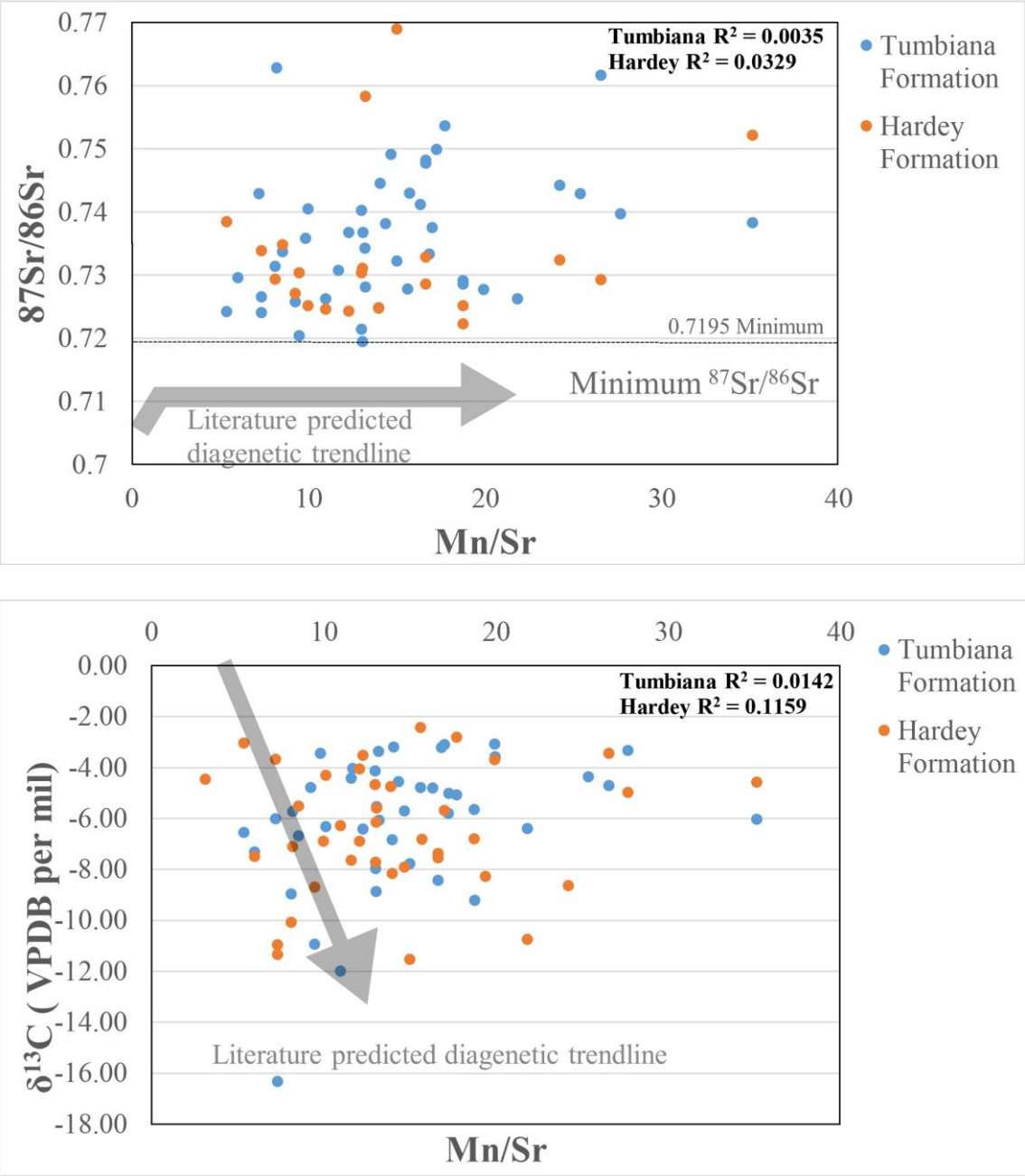

Figure 9: A cross plot of Sr isotopes and Mn/Sr ratios, to test for diagenetic trends, showing also the minimum or least altered $^{87}Sr/^{86}Sr$ values for a local basin/ lake waters. Any values following the linear trend towards higher Mn/ Sr and more radiogenic are more $^{87}Sr/^{86}Sr$ are likely to be diagenetically altered.

The results indicate that the diagenesis plot (Sr isotopes vs Mn/Sr) does not show any obvious trend as indicated in Figure 9. This indicates little to no obvious correlation, which is likely related to complex diagenetic history of these samples and/ or the fact that we are dealing with a lacustrine system rather than marine system, for which

diagenetic trends are poorly understood and can differ from those shown in Figure 8 (Banner & Hanson, 1990; Swart 2015).

Clay contamination is another issue which can introduce false and misleading signals into the carbonate leachate, and in this study this was minimised with sequential leaching to avoid contamination from detrital or clay mineral phases. However to evaluate that no clay mineral phases were present, the Al concentration can be plotted against $^{87}Sr/^{86}Sr$. Additionally, to check for clay contamination there should be an examination of $^{87}Sr/^{86}Sr$ ratios vs Rb/Sr ratios. A high Rb/Sr ratio would indicate a strong radiogenic component likely from clays and thus also highly correlated $^{87}Sr/^{86}Sr$ and Rb/Sr data. As seen in Figure 10, there is a slight trend in both indices for clay contamination (Al and Rb/Sr), when plotted against Sr isotopes (even for corrected values), which indicate likely clay contamination in several of our leached samples. These samples which were strongly correlating and had high radiogenic $^{87}Sr/^{86}Sr$ signals were not considered during interpretations of primary isotope signals in studied rocks.

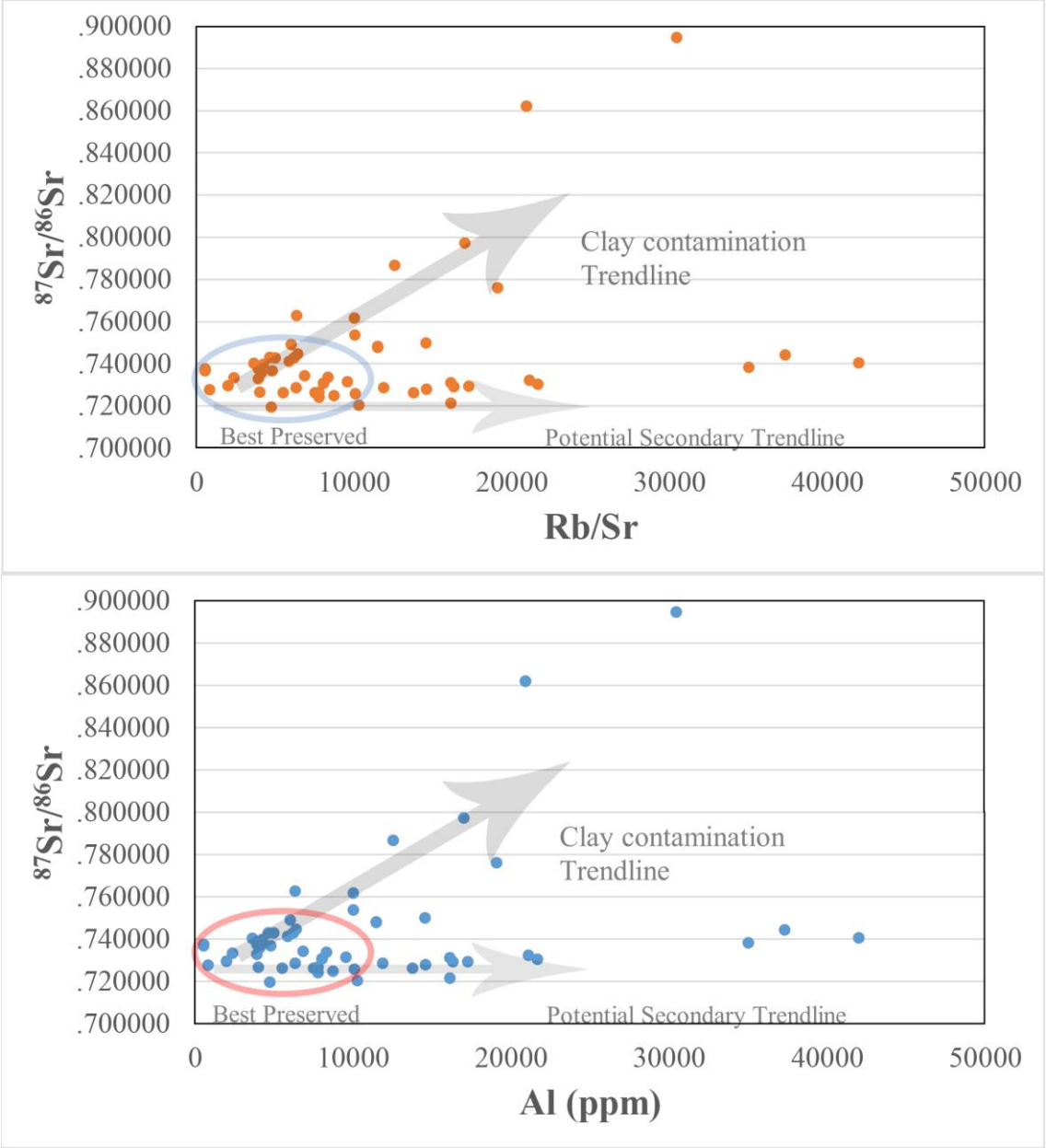

Figure 10: Two different elemental plots to determine clay contamination. Any point following a linear correlation shows potential for clay contamination. The larger the value, the larger the contamination. The largest of these have been taken out of the analysis.

Sr and C isotope constraints on palaeo-depositional environment of Tumbiana and Hardey Formation carbonates

As discussed earlier, the debate as to whether this system was a lacustrine or marine environment at deposition has been in dispute with research providing evidence to support both hypothesis. To support our hypothesis, that it is a lacustrine environment, we can look at the Sr and C isotopic signals to determine deposition. For the $^{87}Sr/^{86}Sr$ ratio, the amount of radiogenic input shown from elevated ^{87}Sr isotopes can indicate the deposition of the carbonate from weathering of Sr from surrounding rock into the water system. As the radiogenic signals should get larger or more radiogenic as it approaches crustal weathering of felsic rocks (compared to mafic and less radiogenic oceanic basaltic rocks), limits can be set on the expected geological environments or bedrocks that contributed to the local weathering signal. For marine environments in the Neoarchean the expected values sit around 0.702, and for restricted basins or lakes with granitic terrains it should be expected that it has a much higher $^{87}Sr/^{86}Sr$, in excess of 0.702.

For $\delta^{13}C$ signals the deposition can be determined by observing how light or heavy these ratios are when standardised to VPDB. For marine sourced signals, the expected values are around zero plus or minus 5 per mil, and for signals with higher volcanic input signals it is expected to show lighter values than -5.

INTERPRETATION OF SR ISOTOPE $^{87}SR/^{86}SR$ TRENDS AND DETERMINING DEPOSITIONAL ENVIRONMENT

The $^{87}Sr/^{86}Sr$ ratios over the two formations allow for some initial assessments in relation to the depositional environment

Before the final interpretations, corrections need to be made for the radiogenic strontium present in the samples from possible in-situ Rb decay. Any ^{87}Rb in the rock that overtime has decayed into ^{87}Sr greatly modifies the ratio of $^{87}Sr/^{86}Sr$ and creates values much higher than expected or that are realistic for primary and unaltered carbonates (Nurgalieva et al., 2007). To correct for Rb in the samples the following equation was used:

$$87Sr/86Sr_{Corrected} = 87Sr/86Sr_{Measured} - (87Rb/86Sr_{Measured} * 1.3972 * 10^{-11}) * (2730 * 10^{6})$$

As seen in Figure 11, most of the very radiogenic$^{87}Sr/^{86}Sr$ data remained high even after Rb correction.

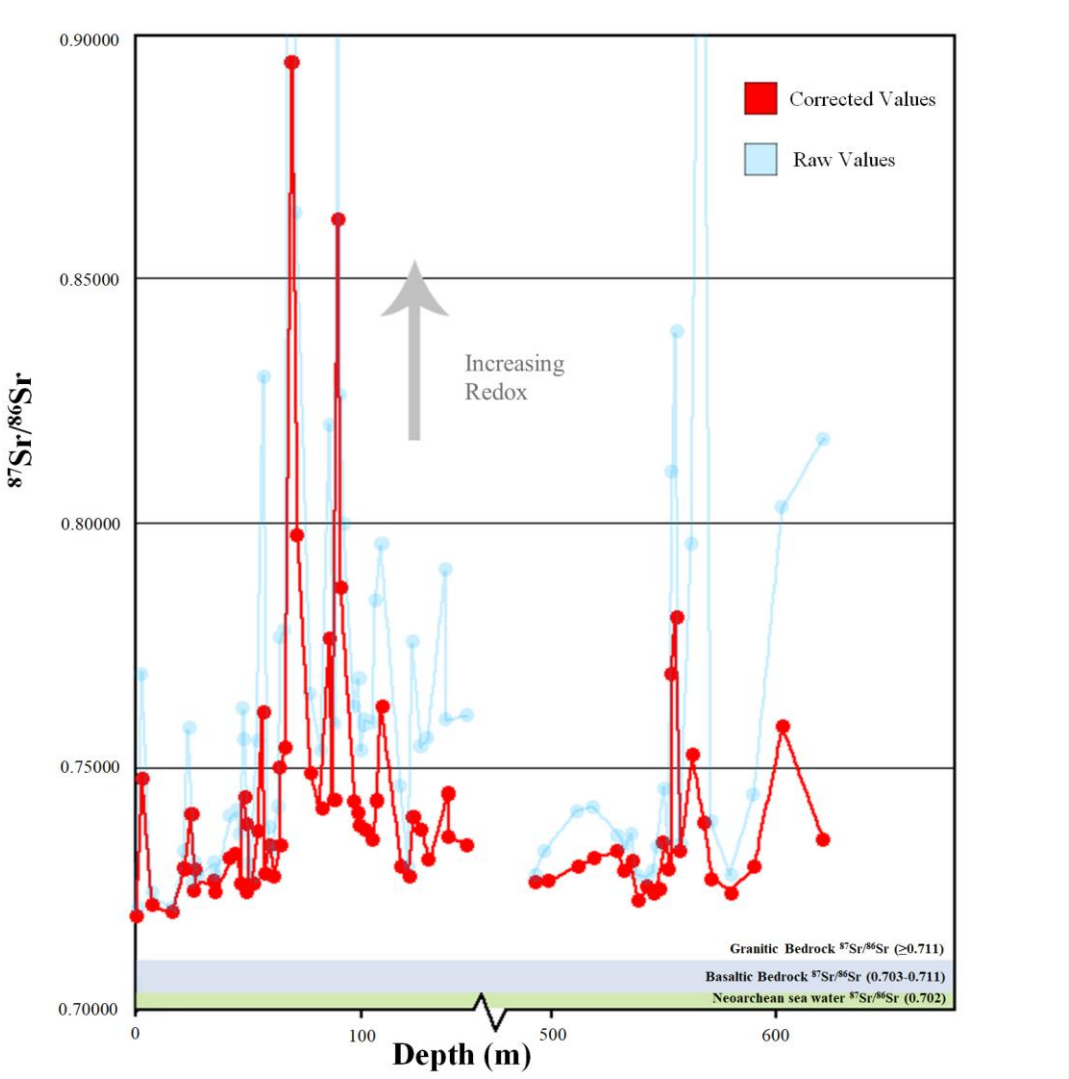

Figure 11: the $^{87}Sr/^{86}Sr$ ratios from both Tumbiana and Hardey Formations. The blue translucent line shows the original unaltered signal, the red solid line being the Rb corrected values. The marine, basaltic, and granitic basin fields are also illustrated.

When looking at the data and determining the $^{87}Sr/^{86}Sr$ ratio for the formations, Figure 9 shows that without the potentially diagenetic samples there is a minimum value in the Tumbiana of ~0.7195, and for the samples from the Hardey Formation the minimum values is ~0.7222. Both of these ratios are far too high and radiogenic if compared to the expected Neoarchean average marine $^{87}Sr/^{86}Sr$ signature of 0.702 - 0.703- (Kuznetsov et al., 2018). When combined with other data, these highly radiogenic signals (even after Rb correction) are able to provide some understanding into the paleo environment, as

such radiogenic nature of the samples is unlikely to be caused by marine or coastal deposition, which in turn suggests continental and presumably lacustrine depositional system. The observed level of radiogenic excess also leads to the assumption that this was not a lake in basaltic terrain, but rather situated near or within granitic/ felsic or some intermediate bedrock lithologies. This is further supported by the high amount of Rb and radiogenic Sr present in the analysed sediments which is an indication of crustal source (Kuznetsov et al., 2018). The increase in $^{87}Sr/^{86}Sr$ that occurs between 60 m to 110 m is potentially due to a further increase in restriction of the basin or lake, reducing any effect of marine water mixing and further increasing the radiogenic $^{87}Sr/^{86}Sr$ ratios. This data, particularly the best preserved signals shown in Figure 10, shows that there is clearly an increase in radiogenic Sr input and that therefore there is evidence to support a lacustrine system and not a marine system. This also agrees with interpretations of (Bolhar & Van Kranendonk, 2007; R. Buick, 1992; Sakurai, Ito, Ueno, Kitajima, & Maruyama, 2005; Stanley & Buchheim, 2009) which supports the lacustrine hypothesis. While the $^{87}Sr/^{86}Sr$ ratios do directly support a lake environment, these ratios are very radiogenic (approaching 0.8-0.9 is some areas). This can be explained by a few different factors. The first factor is the presence of felsic to intermediate surrounding geology/bedrock (Stromberg, Spinks, & Pearce, 2019) which has been weathered into the hypothetical lake system which largely increases the radiogenic Sr signal as seen in Figure 12.

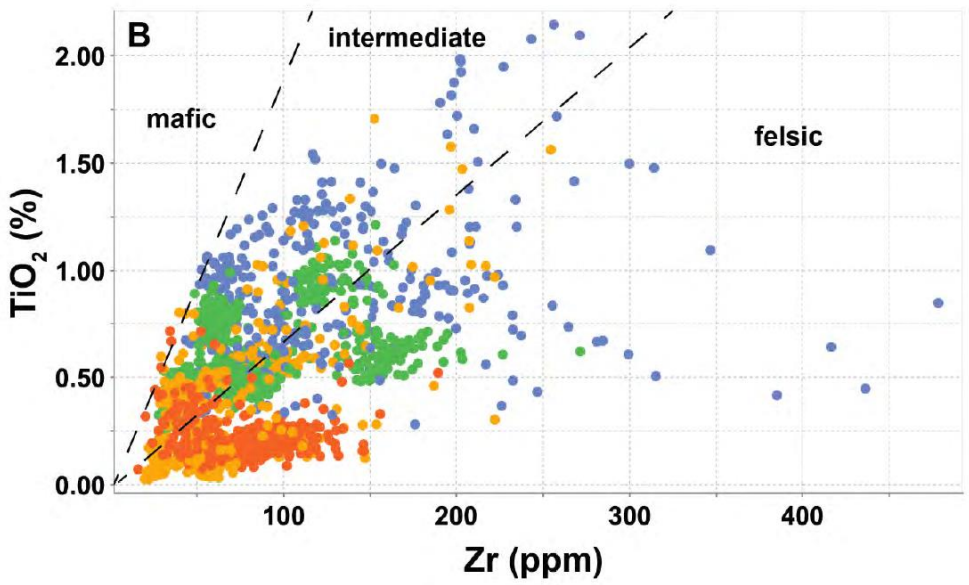

Figure 12: The bulk geochemical analysis of source rock material performed on the whole 18ABAD01 core by CSIRO (Stromberg, Spinks, & Pearce, 2019)

Secondly we also have the presence of in-situ decay of Rb to Sr, which due to the age of the rocks impacts the $^{87}Sr/^{86}Sr$ ratios of the rock a lot more than a younger rock, due to the ^{87}Rb half-life age of 48.8 Ga. The correction applied to the rocks for in-situ Rb decay did bring down the ratios, however would not have accounted for 100% of decayed Rb.

Finally the potential detrital and clay contamination of the carbonates could additionally increase the radiogenic signal due to the higher amount of radiogenic Sr and Rb found in clays.

INTERPRETATIONS OF CARBON ISOTOPE $\Delta^{13}C$ RECORD: PHOTOSYNTHESIZERS VS METHANOGENS

The $\delta^{13}C$ as seen in Figure 13, is separated into the two formations of interest, the first of which is the Tumbiana Formation.

The Tumbiana Formation starts at a $\delta^{13}C$ of -8 per mil at its youngest age and trends up over the next 145m to -3.37 per mil. This trend of lighter isotopes indicates that the Tumbiana is not a marine setting and indicates a carbon input from lighter $\delta^{13}C$ sources. However the signal is still not definitively outside the region of marine and so it can't be completely excluded. This lighter carbon source is possibly from a volcanic source (volcanic CO_2) as the common $\delta^{13}C$ for a magmatic carbon signal is approximately between -5 to -7 per mil (Mattey, 1987).

The notable exception is found at depths 100m to 120m where the $\delta^{13}C$ signal becomes lighter at range -5.5 to -7.3 per mil. This short-lived change could be an indication of a slight variation in environment and when compared to the lithology seen in Figure 14 there is a correlation between this region and the existence of stromatolites. The implication of this data suggests that early in the Tumbiana there were inputs from an organic carbon source which drives the $\delta^{13}C$ below a typical Archean marine signal (although this would not be applicable to lacustrine systems). As the signal becomes more negative, the $\delta^{13}C$ source seems to come from an increasing amount of volcanic sourced CO2 as the production of the organic carbon seems to decrease. Another light C isotope excursion is present at around the 35m depth. This is a region where the source

rocks are quite low in carbonate percentage and the presence of other chemical processes during formation could explain the alteration of these signals.

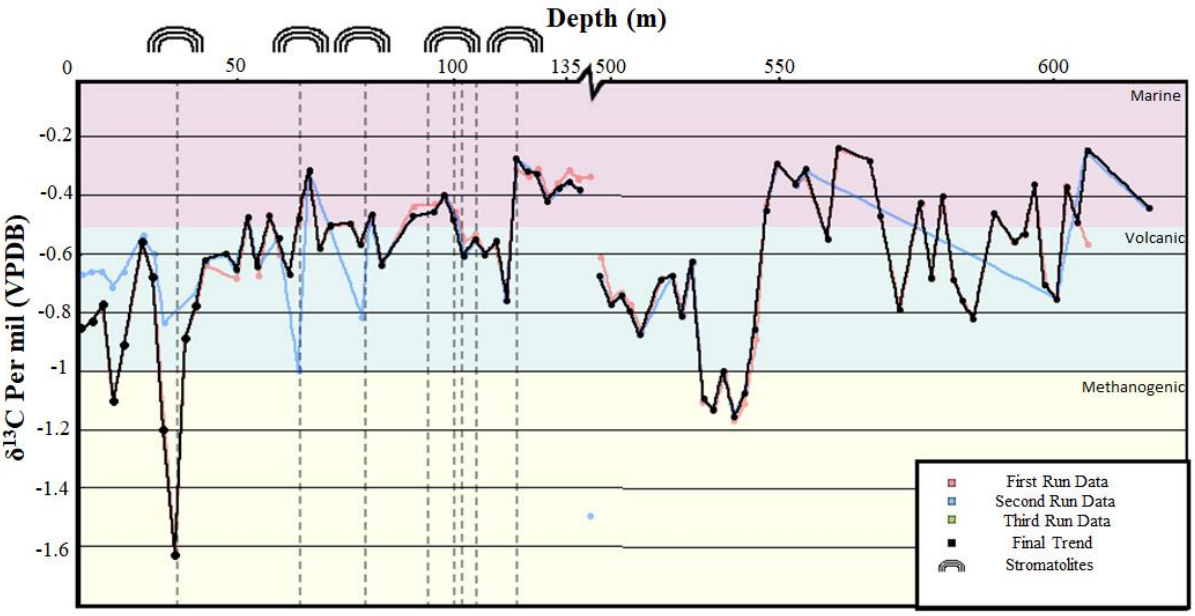

Figure 13: $\delta^{13}C$ isotope plot with defined areas for different carbon inputs. Through the Tumbiana Formation, the lithological stromatolites have been marked with dashed lines indicating their depth (Stromberg et al., 2019).

The Hardey Formation data also indicates sourcing from potentially non-marine settings, with values ranging from about -4 to -8 per mil. Once again, these signals are very negative compared to a marine setting but still lie within its bounds and show the potentially variations due to volcanic input. However, there is a period between 525m and 548m which shows an extremely light indication of $\delta^{13}C$ which cannot be accounted for by volcanic input (as these values are much lower than volcanic $\delta^{13}C$ of about -5 to -6 per mil). Instead these values are potential indicators of methanogenesis, which is due to the very light carbon in methane being produced from some of the first bacterial life on Earth. This process turns CO_2 to CH_4 instead of the more commonly known O_2 producing photosynthetic cyanobacteria. This change in $\delta^{13}C$ due to methane production

is the only known geochemical process which can cause a significant $\delta^{13}C$ depletion (Schoell & Wellmer, 1981).

The C isotopes shown in Figure 13 do not completely rule out a marine environment (shown from overlaps between expected marine and the volcanic $\delta^{13}C$) but this data set also does not disprove a lacustrine setting. However, there is evidence of extremely negative $\delta^{13}C$ methanogenic suggested signals present in the Hardey Formation and another set of signals based in the Tumbiana Formation suggesting the presence of oxygen producing life as seen correlating in both Figure 13 and Figure 14.
Based on this sedimentary record and C isotopic signal, it is possible to begin to observe a transition over time between a methanogen-dominated ecosystem (low $\delta^{13}C$ and no stromatolites) to a more cyanobacterial and photosynthetic-dominated environment (higher $\delta^{13}C$ with stromatolites.

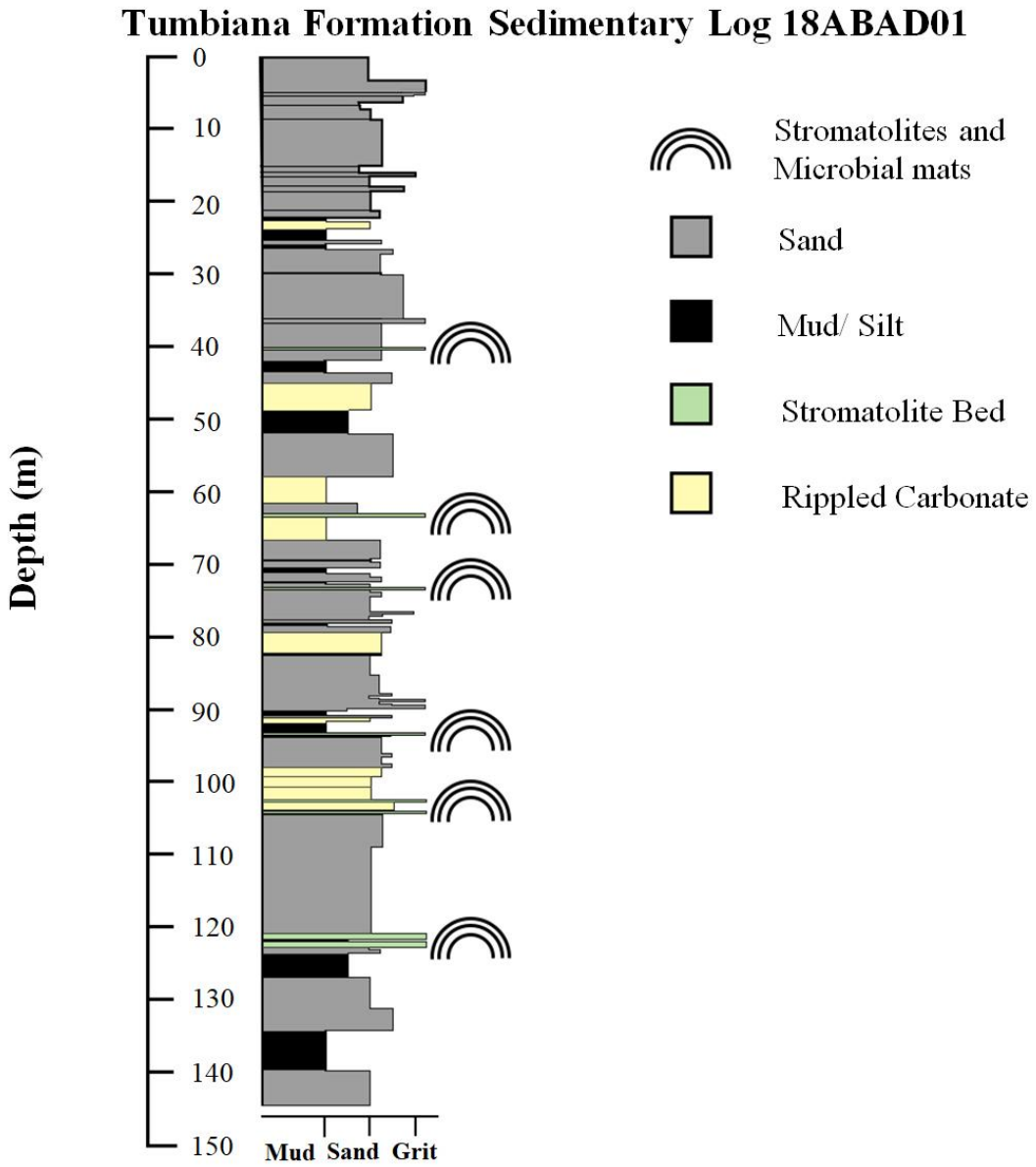

Figure 14: Downhole Lithology of the Tumbiana Formation of 18ABAD01. The noted sedimentary structures are stromatolites, ooid beds, slumps, soft sedimentary deformation and desiccation/syneresis cracks (modified from Stromberg, Spinks, & Pearce, 2019).

The combination of both the $^{87}Sr/^{86}Sr$ ratios, the $\delta^{13}C$ data and the stratigraphic and sedimentological record provides strong basis to conclude that during the deposition the Tumbiana Formation local carbonates were formed in a lacustrine system, perhaps with some but minimal level of marine interactions, which however cannot be proved by our

data. Such lacustrine settings and restriction are shown in the increase in radiogenic Sr isotope signal, with the shallowing shown through the presence of stromatolites which are restricted to shallower waters, changing to less restricted as time went on. There is also evidence to support the transition between the Hardey and Tumbiana Formation of methanogens to photosythesisers present in an early restricted basin or lake.

If there was a restriction in the presence of stromatolites, then the next step would be to check for any presence of local oxygenation occurred in this lacustrine environments due to these photosynthetic bacteria.

Cr isotope and trace element (Zn/Fe and REE) constraints on palaeo-redox conditions of Tumbiana and Hardey Formation carbonates

To understand changes in palaeo-redox and past atmospheric O_2 levels, one can apply a multi-proxy approach based on Cr isotopes, REE and Zn/Fe ratios. By measuring changes in these palaeo-redox proxies we can infer past atmospheric O_2 conditions and marine redox. As to REE, Cerium can be used as redox sensitive element which is able to exist in oxidations states 3+ and 4+. When in oxic conditions it oxidises from 3+ to 4+ and adsorbs onto surface material, this causes removal of Ce from the water column, reflected as negative Ce anomalies.

To measure such Ce anomalies, the Ce present in ppm is normalised against PAAS (Post Archean Australian Shales) (Taylor & McLennan, 1985) and the REE either side of Ce. If any negative anomaly is present this can indicate the presence of oxic conditions in a marine environment, however this result may not always be present in a lake environment as the suit of REE can be easily disturbed and complicated by other processes which are poorly understood and unconstrained.

On the other hand, use of other palaeo-redox proxies like $\delta^{53}Cr$ show oxic conditions through positive $\delta^{53}Cr$ excursions due to oxidative weathering and so this tracer is likely more reliable also in lacustrine systems compared to Ce anomalies.

RARE EARTH ELEMENTS AND CERIUM ANOMALIES

Before the samples can be analysed, a comparison between the Ce anomalies with the Pr normalised in the same manner.

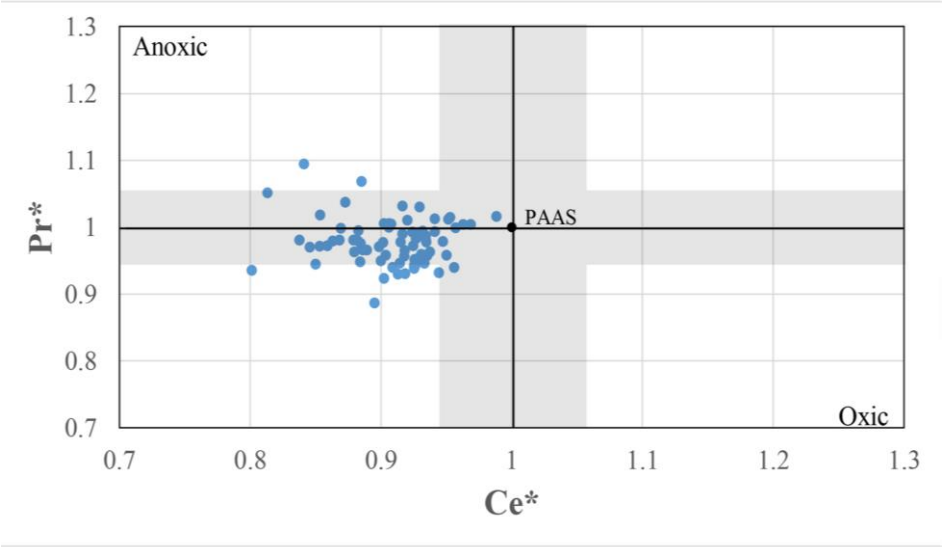

Figure 15: Figure of the Ce* anomaly. The Ce* vs Pr* where the signal is mainly in the undetermined region of error.

When plotted Ce/Ce* and Pr/Pr* (for calculation see Appendix B) against each other one can determine that most values from the samples fall in the “anoxic” region (defined by positive Ce anomalies) or in the La anomaly region (bottom right), see Figure 15. Similarly, in Figure 5, the REY (Rare Earth Element and Yttrium) pattern shows no characteristic negative Ce anomaly or positive Y anomaly usually seen in sea

water (Tostevin et al., 2016). This second piece of information is valuable as a lack of marine characteristic REY signals provides further evidence of non-marine and thus lacustrine deposition. The lack of a Ce anomaly for redox conditions is not a guaranteed method as the Ce may have been deposited in oxic waters with no Ce anomaly and Ce also has limitations in resolution around restricted settings (Tostevin et al., 2016).

Zn/Fe Ratios as a palaeo-redox proxy

Another redox proxy that can applied is based on elemental Zn/Fe ratios, see Figure 16. In anoxia we expect that the ratio of Zn and Fe to be stable. This ratio however will change with the change to oxic conditions where Zn^{2+} remains divalent and Fe^{2+} is oxidised to Fe^{3+}. With this oxidation, Fe will start to precipitate as Fe_2O_3, this will shift the ratio showing a change in the Zn/Fe signal (Liu et al., 2015). This ratio as a proxy functions as an indicator based of the following assumptions: the source of Zn and Fe is predominantly from hydrothermal inputs, the Fe and Zn are similarly soluble in oceans, the partition coefficient for Zn/Fe is unchanging, and the oxidised Fe is precipitated and not taken into carbonate.

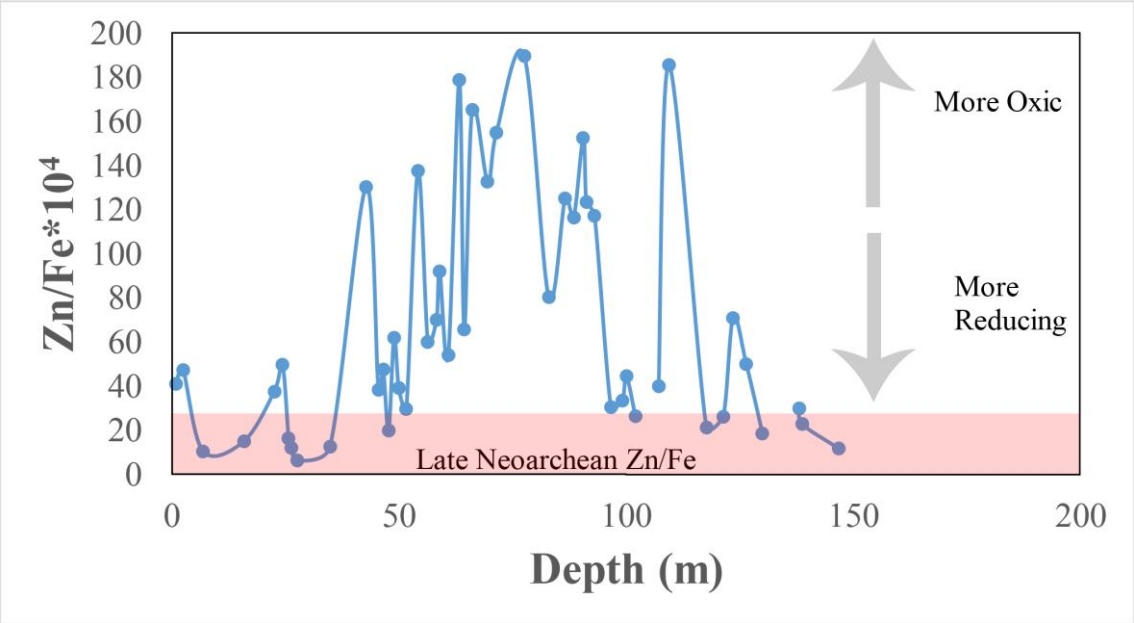

Figure 16: The Zn/Fe ratios over the Tumbiana Formation. Marked are the general values expected for the Neoarchean from literature (Liu et al., 2015), this trend shows a curve much higher than the expected anoxic ratios.

This higher Zn/Fe ratio is an indication of a redox change towards more oxic conditions present at depth from 60m to 125m, further indicating that redox changes removed Fe from water likely due to presence of local oxic water. This same trend correlates lithologically with the presence of stromatolites, as well as the restricting of the basin/ lake based on Sr isotope data.

δ^{53}Cr as palaeo-redox proxy

Chromium is another redox element to check for change in oxygen levels. As Cr has four stable isotopes, the two most abundant (^{52}Cr and ^{53}Cr) can be used to trace changes in redox conditions and thus oxygen levels through geologic time. This is due to the two valence states of Cr^{3+} and Cr^{6+} that allows mobility and Cr isotope fractionation during redox cycling of Cr (Li et al., 2016). As seen in Figure 17, there is a distinct rise in

$\delta^{53}Cr$ at the same depths at which Zn/Fe rises. Both proxies point to a relatively more oxic local condition during deposition of these carbonates also dominated by the occurrence of stromatolites (i.e., photosynthetic O_2 production) and more radiogenic Sr isotope values (i.e., restriction). This rise in $\delta^{53}Cr$ indicates the local environment was conducive to oxygenation of the local water where O_2 could build up in shallow lake waters over a long enough period to produce such pronounced redox signal.

This potentially indicates that as the basin or lake became more restricted, the conditions were also more favourable to stromatolitic growth that in turn produced local input of oxygen into the system. When compared to global literature data set, this clearly shows that there is an anomaly in oxygen during the Neoarchean, see Figure 18 & 19.

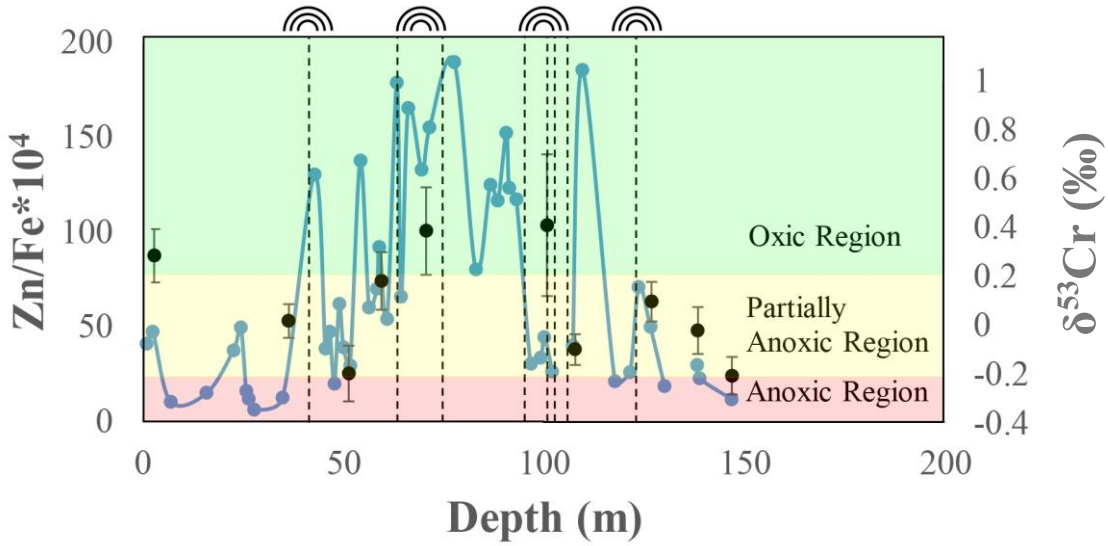

Figure 17: Results from the Tumbiana Formation with Zn/Fe ratios overlain with $\delta^{53}Cr$ values. The dashed lines represent the lithological stromatolites found in the 18ABAD01 core.

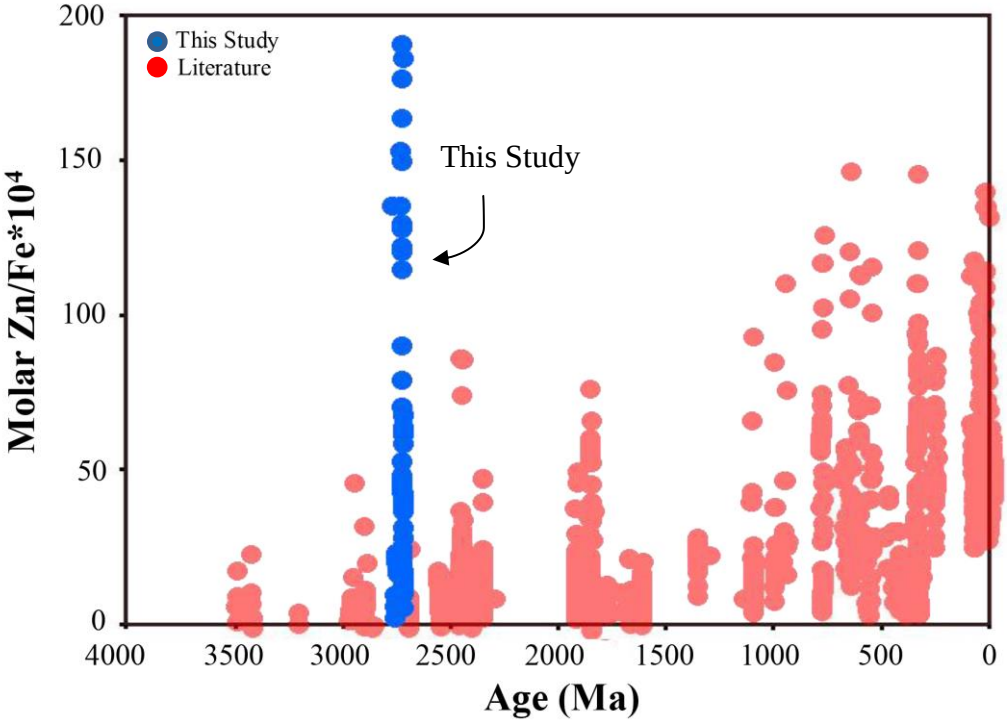

Figure 18: The global Zn/Fe data trend based on marine carbonates (modified from Liu et al., 2015), compared to the data from 18ABAD01 (this study) showing Zn/Fe values much greater than expected for marine settings during Archean times.

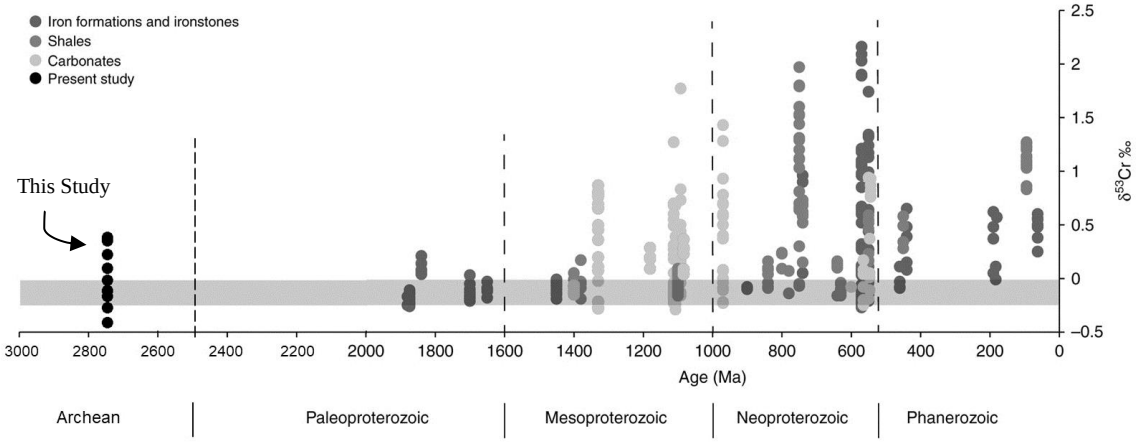

Figure 19: The global δ53Cr data trend over the last 2000 Ma, the grey bar represents the crustal value (modified from Canfield et al., 2018).

Implications for applied research and mineral exploration

Implications of redox change in a restricted environment has implications for future mineral exploration. As changes in oxidation can lead to precipitation and mobilisation of elements (Borch et al., 2010), investigations can examine whether this local change in oxygen levels impacted the surrounding rock formations.

There is evidence suggesting potential mineralisation in the Kylena Formation and base of the Tumbiana Formation generated from airborne electromagnetic surveys imaging shallow conductive base metals which were taken in the area. Further geochemistry of the surrounding rock found elevated Zn, Pb and Cu. Cu anomalies were found in the base of the Tumbiana Formation in the form of vein hosted Cu, with evidence of white micas and low temperature alteration present in the rock formation. This evidence points to the possibility of Stratiform Sedimentary hosted Cu (SSC) (Stromberg et al., 2019).

An SSC is a mineral deposit characterised by the following traits: containing ore body horizons at boundaries of oxidation and reduction, stratified mineralisation to specific beds, compositions of fine grained Cu-sulfides and Pb-Zn, Ag and Co, clearly visibly lateral and vertical sulphide zonation, and no direct evidence of volcanic activity within deposit. Typical ore fluids are believed to have been derived from underlying sediments containing volcanics and/ or igneous bodies (Misra, 2000).

While SSC mineral deposits have been reported in the area, this is much older than has been previously globally reported. The earliest reported SSC deposit was dated at ~2 Ga, see Figure 20.

As SSC deposits require oxic meteoric water to transport and concentrate Cu, the potential for a deposit was not investigated past the age 2 Ga due to lack of oxic waters available during this period (Misra, 2000).

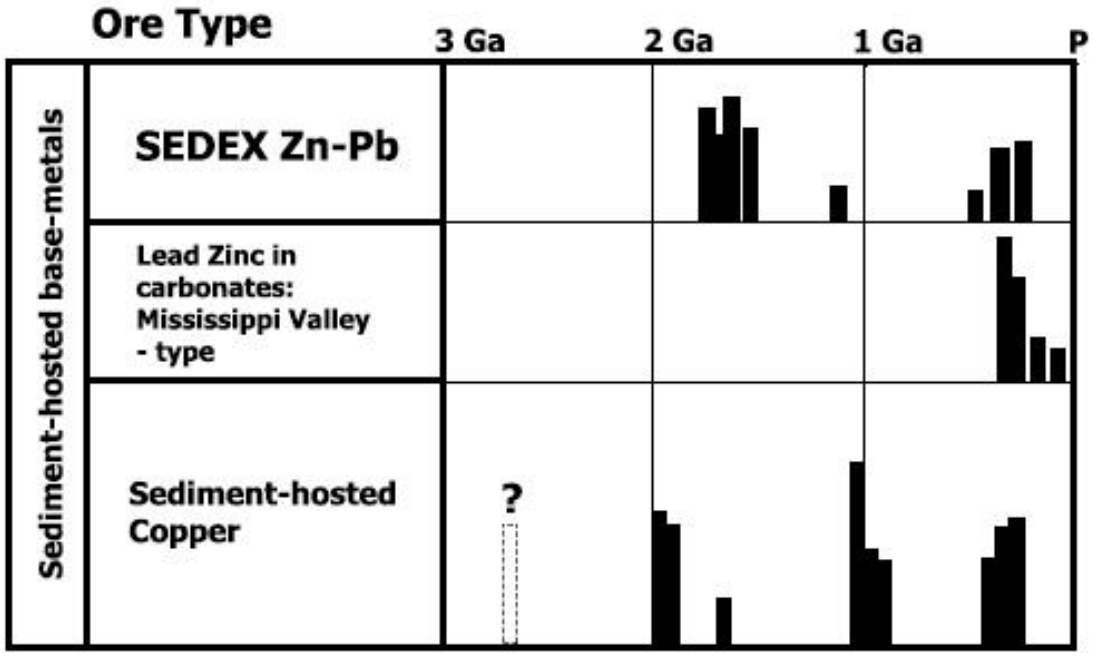

Figure 20: Previous mineralisation's known in literature. These all end at ~2 Ga, due to the lack of oxygen SSC deposits were not thought to have existed in the Archean (modified from Groves, Vielreicher, Goldfarb, & Condie, 2005).

This mineralisation system proposes meteoric drainage water, interacted with the oxic water from the stromatolitic restricted basin and mobilised Cu in the surrounding rock and as the heat from the basin causes the water to rise into the surrounding sediments it precipitated the Cu (Bornhorst & Mathur, 2017).

A proposed mechanism for how Cu is concentrated into a SSC deposit in the Tumbiana Formation can be seen in Figure 21.

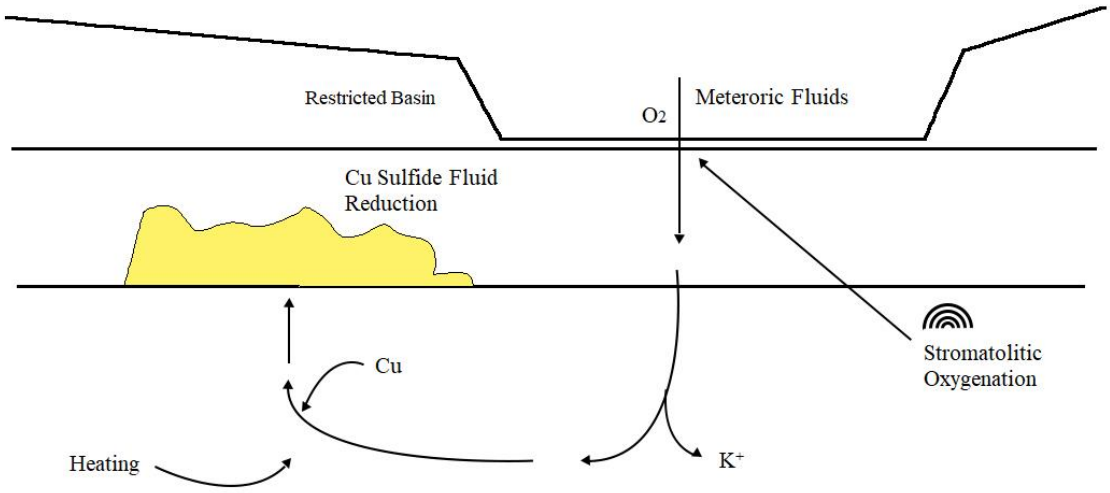

Figure 21: The proposed mineralisation system for the Fortescue Group showing the concentration of Cu at a redox boundary. Adapted from (Stromberg, Spinks & Pearce, 2019).

Due to this study, this proposed deposit provides a strong argument for how the deposit could exist outside reported range of past SSC deposits. Thanks to the unique nature of this restricted stromatolite basin, oxygenation occurs in local water to form these deposits. This indicates that the basin is the source of one of the earliest known SSC deposits (Groves et al., 2005).

CONCLUSIONS

Using $^{87}Sr/^{86}Sr$ and $\delta^{13}C$ in the 18ABAD01 core the depositional environment of the Neoarchean Tumbiana Formation has been constrained. Results from very radiogenic $^{87}Sr/^{86}Sr$ suggests a restriction and lacustrine setting with very radiogenic and non-marine Sr isotope signals (even after corrections for in-situ Rb decay) in the Tumbiana Formation which coincides with the presence of stratigraphically correlating stromatolites. While the $\delta^{13}C$ doesn't confirm lacustrine, it is not conclusive of a marine setting. The $\delta^{13}C$ did however display a transition between methanogenic and photosynthetic processes across the Hardey and Tumbiana Formation which also correlates with the stratigraphic log.

Using REE, trace and major elements and $\delta^{53}Cr$ in the same core the palaeo-redox environment of the Tumbiana Formation has been constrained. REE were unable to show either oxia or anoxia via Ce negative anomalies due to non-marine deposition making it difficult to determine redox. The Zn/Fe data strongly supports evidence for a period of oxic conditions over the depths of 60m to 125m and also associates with the occurrence of stromatolites during the Tumbiana Formation. The $\delta^{53}Cr$ similarly shows evidence supporting local oxidation and active redox cycling of Cr during deposition of the Tumbiana Formation and correlates with the similar trends of the Zn/Fe data.

This data provides strong evidence to suggest that during the deposition of the Tumbiana Formation there was a local oxygen rich environment in a restricted lacustrine setting which was weathered from intermediate to felsic material. Our

Palaeo-redox constraints support conditions with locally oxidised waters, which are conducive for copper mobilisation during oxic water drainage, with implications also for accumulation of Cu in sediment-hosted stratiform copper (SSC) deposits.

ACKNOWLEDGMENTS

I personally would like to first and foremost thank Juraj Farkas for his help and guidance on this project, his knowledge and input was invaluable. I would like to also thank my secondary supervisors Sam Spinks and Alan Collins, Sam's insight into the Fortescue and Alan's knowledge on anything and everything was extremely helpful. I'd like to thank CSIRO and Artemis Resources for access the drill core this paper was based on, allowing me to view their data and their funding. I'd like to thank David Bruce, for putting up with the massed horde of honours students rampaging through his lab and still finding time to help. I'd also like to thank Rob Klaebe for his vast knowledge on Chromium isotopes and his very insightful discussions. I'd like to thank Sarah Gilbert and Adelaide Microscopy for helping me run my ICP data. Finally, I'd like to thank my honours cohort for their support during the year and particularly Josh Watson and Savannah Liebelt for keeping company during late lab nights and helping answer questions when no one else was around.

REFERENCES

Banner, J. L., & Hanson, G. N. (1990). Calculation of simultaneous isotopic and trace element variations during water-rock interaction with applications to carbonate diagenesis. *Geochimica et Cosmochimica Acta, 54*(11), 3123-3137. doi: 10.1016/0016-7037(90)90128-8

Bolhar, R., & Van Kranendonk, M. J. (2007). A non-marine depositional setting for the northern Fortescue Group, Pilbara Craton, inferred from trace element geochemistry of stromatolitic carbonates. *Precambrian Research, 155*(3), 229-250. doi: 10.1016/j.precamres.2007.02.002

Borch, T., Kretzschmar, R., Kappler, A., Cappellen, P. V., Ginder-Vogel, M., Voegelin, A., & Campbell, K. (2010). Biogeochemical Redox Processes and their Impact on Contaminant Dynamics. *Environmental Science & Technology, 44*(1), 15-23. doi: 10.1021/es9026248

Bornhorst, T. J., & Mathur, R. (2017). Copper Isotope Constraints on the Genesis of the Keweenaw Peninsula Native Copper District, Michigan, USA. *minerals*.

Buick, R. (1992). The antiquity of oxygenic photosynthesis: Evidence from stromatolites in sulphate-deficient Archaean lakes. *Science, 255*(5040). doi: 10.1126/science.11536492

Buick, R. (1992). The antiquity of oxygenic photosynthesis: evidence from stromatolites in sulphate-deficient Archaean lakes. *Science, 255*(5040), 74-77. doi: 10.1126/science.11536492

Canfield, D. E., Zhang, S., Frank, A. B., Wang, X., Wang, H., Su, J., . . . Frei, R. (2018). Highly fractionated chromium isotopes in Mesoproterozoic-aged shales and atmospheric oxygen. *Nature Communications, 9*(1), 2871. doi: 10.1038/s41467-018-05263-9

Coffey, J. M., Flannery, D. T., Walter, M. R., & George, S. C. (2013). Sedimentology, stratigraphy and geochemistry of a stromatolite biofacies in the 2.72 Ga Tumbiana Formation, Fortescue Group, Western Australia. *Precambrian Research, 236*, 282-296. doi: 10.1016/j.precamres.2013.07.021

Database, A. S. U. (1988). Nickol River Formation. from Geoscience Australia

Grey, K. (2009). *Microbialites of Lake Thetis, Cervantes, Western Australia : a field guide / K. Grey and N.J. Planavsky*. East Perth, W.A: Geological Survey of Western Australia.

Groves, D. I., Vielreicher, R. M., Goldfarb, R. J., & Condie, K. C. (2005). Controls on the heterogeneous distribution of mineral deposits through time. *Geological Society Special Publication, 248*(1), 71-101. doi: 10.1144/GSL.SP.2005.248.01.04

Gumsley, A. P., Chamberlain, K. R., Bleeker, W., Söderlund, U., de Kock, M. O., Larsson, E. R., & Bekker, A. (2017). Timing and tempo of the Great Oxidation Event. *Proceedings of the National Academy of Sciences of the United States of America, 114*(8), 1811. doi: 10.1073/pnas.1608824114

Hall, C. (2005). SHRIMP U–Pb depositional age for the lower Hardey Formation: evidence for diachronous deposition of the lower Fortescue Group in the southern Pilbara region, Western Australia. *Australian Journal of Earth Sciences, 52*(3), 403-410. doi: 10.1080/08120090500134506

Hodgskiss, M. S. W., Crockford, P. W., Peng, Y., Wing, B. A., & Horner, T. J. (2019). A productivity collapse to end Earth's Great Oxidation. *Proceedings of the National Academy of Sciences, 116*(35), 17207-17212. doi: 10.1073/pnas.1900325116

Johnson, J. E., Gerpheide, A., Lamb, M. P., & Fischer, W. W. (2014). O2 constraints from Paleoproterozoic detrital pyrite and uraninite. *GSA Bulletin, 126*(5-6), 813-830. doi: 10.1130/b30949.1

Kuznetsov, A., Semikhatov, M., & Gorokhov, I. (2018). Strontium Isotope Stratigraphy: Principles and State of the Art. *Stratigraphy and Geological Correlation, 26*(4), 367-386. doi: 10.1134/S0869593818040056

Li, C.-F., Feng, L.-J., Wang, X.-C., Chu, Z.-Y., Guo, J.-H., & Wilde, S. A. (2016). Precise measurement of Cr isotope ratios using a highly sensitive Nb 2 O 5 emitter by thermal ionization mass spectrometry and an improved procedure for separating Cr from geological materials. *J. Anal. At. Spectrom., 31*(12), 2375-2383. doi: 10.1039/c6ja00265j

Liu, X.-M., Kah, L., Knoll, A., Cui, H., Kaufman, A., Shahar, A., & Hazen, R. (2015). Tracing Earth's O2 evolution using Zn/Fe ratios in marine carbonates. *Geochemical Perspectives Letters, 2*, 24-34. doi: 10.7185/geochemlet.1603

Mattey, D. P. (1987). *Carbon isotopes in the mantle* (Vol. 7): Terra Cognita.

Misra, K. C. (2000). Sediment-Hosted Stratiform Copper (SSC) Deposits *Understanding Mineral Deposits* (pp. 539-572). Dordrecht: Springer Netherlands.

Nurgalieva, N., Ponomarchuk, V., & Nourgaliev, D. (2007). Strontium isotope stratigraphy: Possible applications for age estimation and global correlation of Late Permian carbonates of the Pechishchi type section, Volga River. *Russian Journal of Earth Sciences, 9*, 1-8. doi: 10.2205/2007ES000221

Packer, B. (1990). Sedimentology, paleontology, and stable isotope geochemistry of selected formations in the 2.7-billion-year-old Fortescue Group, western Australia. In R. V. Ingersoll (Ed.): ProQuest Dissertations Publishing.

Sakurai, R., Ito, M., Ueno, Y., Kitajima, K., & Maruyama, S. (2005). Facies architecture and sequence-stratigraphic features of the Tumbiana Formation in the Pilbara Craton, northwestern Australia: Implications for depositional environments of oxygenic stromatolites during the Late Archean. *Precambrian Research, 138*(3-4), 255-273. doi: 10.1016/j.precamres.2005.05.008

Schoell, M., & Wellmer, F. W. (1981). Anomalous 13C depletion in early Precambrian graphites from Superior Province, Canada. *Nature, 290*(5808), 696. doi: 10.1038/290696a0

Shields, G., & Veizer, J. (2002). Precambrian marine carbonate isotope database: Version 1.1. *Geochemistry, Geophysics, Geosystems, 3*(6), 1 of 12-12 of 12. doi: 10.1029/2001GC000266

Sosa Torres, M. E., Saucedo-Vázquez, J. P., & Kroneck, P. M. H. (2015). The Magic of Dioxygen. In P. M. H. Kroneck & M. E. Sosa Torres (Eds.), *Sustaining Life on Planet Earth: Metalloenzymes Mastering Dioxygen and Other Chewy Gases* (pp. 1-12). Cham: Springer International Publishing.

Stanley, A., & Buchheim, P. (2009). A giant, Late Archean lake system: The Meentheena Member (Tumbiana Formation; Fortescue Group), Western Australia. *Precambrian Research, 174*, 215-240. doi: 10.1016/j.precamres.2009.07.005

Stromberg, J., Spinks, S., & Pearce, M. (2019). Geochemical Stratigraphy of the Neoarchean Lower and Middle Fortescue Group, Western Australia (C. M. Resources, Trans.). CSIRO Mineral Resources: CSIRO Mineral Resources.

Taylor, S. R., & McLennan, S. M. (1985). *The Continental Crust: its Composition and Evolution*: Blackwell Scientific Publications.

Thorne, A. M. T., AF. (2001). Geology of the Fortescue Group, Pilbara Craton, Western Australia. *Bulletin 144, 144*, 249.

Tostevin, R., Shields, G. A., Tarbuck, G. M., He, T., Clarkson, M. O., & Wood, R. A. (2016). Effective use of cerium anomalies as a redox proxy in carbonate-dominated marine settings. *Chemical Geology, 438*(C), 146-162. doi: 10.1016/j.chemgeo.2016.06.027

Van Kranendonk, M., Hickman, A., Smithies, R. H., Nelson, D., & Pike, G. (2002). Geology and tectonic evolution of the archean North Pilbara terrain, Pilbara Craton, Western Australia. *Econ. Geol. Bull. Soc. Econ. Geol., 97*(4), 695-732. doi: 10.2113/gsecongeo.97.4.695

APPENDIX A: EXTENDED METHODS

QQQ-ICP-MS

The conditions required for work on the Agilent 8900x QQQ-ICP-MS and its plasma conditions are: RF power 1550W, sample depth of 8mm and Ar carrier gas flow rate of 1.09 L/min, with a Micro Mist nebuliser and Scott Type spray chamber. The collision cell was run in He mode (4mL/min He gas flow) for the majority of the elements (Mg, Al, Sc, Ti, V, Cr, Mn, Co, Ni, Cu, Zn, Ga, Rb, Y, Zr, Nb, Mo, Cd, Cs, Ba, Hf, Ta, Pb, Th, U and all REE). P, Ca, Fe were analysed with Oxygen (30% flow rate) in the collision cell and the MO+ reaction products measured each element and were higher by atomic weight of 16 for the added O. The internal standard In was used for instrumental drift and calibrated solutions of mixed solutions (0, 10, 20, 50, 100, 200 and 500 ppb) were used for quantifying. JDo-1 and JLs-1 were used as controls for quality of data.

Tungsten Ring Mill

Samples powdered for Cr analysis were milled using Rocklabs tungsten carbide ring mill for 30 seconds to achieve a smooth powder devoid of grit. The standard cleaning procedure for milling was to mill quartz grains for a minute and cleaning with ethanol between each sample to ensure no contamination.

$^{50\text{-}54}$Cr Double Spike

The amount of double spike added to each sample was calculated based on the concentrations from ICPMS data. The double spike was added before the first leaching acid was used to account for possible loss of Cr and δ^{53}Cr fractionation occurring during leaching and purification. This means the double spike is representative of the Cr present in the rock instead of values derived from leaching and purification

TIMS

To account for ^{50}V interference in ^{54}Cr, IUPAC ^{49}Ti/^{50}Ti values of 1.04320 and ^{50}V/^{51}V values of 0.002503 were used to correct ^{54}Cr. To account for ^{54}Fe interference, IUPAC ^{54}Fe/^{56}Fe values of 0.063703.

APPENDIX B: CALCULATIONS

REE anomaly calculations:

The Post-Archean Average Australian Shale (PAAS) normalised cerium anomalies (Ce/Ce*) were calculated based on equations from (G.E. Webb & Kamber, 2000).

$$Ce/Ce^* = [Ce/Ce_{(PAAS)}] / [0.5 \times (La/La_{(PAAS)}) + 0.5 \times (Pr/Pr_{(PAAS)})]$$

The PAAS normalised praseodymium anomalies (Pr/Pr*) was calculated using the same equation modified for Pr's position on the periodic table.

$$Pr/Pr^* = [Pr/Pr_{(PAAS)}] / [0.5 \times (Ce/Ce_{(PAAS)}) + 0.5 \times (Nd/Nd_{(PAAS)})]$$

The PAAS values used in the former equations are REE composition values shown below based on (Nance & Taylor, 1976).

REE	La	Ce	Pr	Nd	Sm	Eu	Gb	Tb	Dy	Ho	Er	Tm	Yb	Lu
PAAS (ppm)	38	80	8.9	32	5.6	1.1	4.7	0.8	4.4	1.0	2.9	0.4	2.8	0.4

In-situ Rb decay Corrections:

The $^{87}Sr/^{86}Sr$ was corrected for in-situ Rb decay by using $^{87}Sr/^{86}Sr$ ratios from the TIMS, $^{87}Rb/^{86}Sr$ ratios from the ICPMS and the age of the carbonate. The calculation is based on (Nurgalieva, Ponomarchuk, & Nourgaliev, 2007).

$$^{87}Sr/^{86}Sr_{(Corrected)} = {}^{87}Sr/^{86}Sr_{(Measured)} - [{}^{87}Rb/^{86}Sr_{(Measured)} * [(1.3972 * 10^{-11}) * Age_{(Years)}]]$$

APPENDIX C: FULL DATA SETS

Table 1: $\delta^{53}Cr$ data set (TIMS), colours accent the $\delta^{53}Cr$ fractionation values and their standard error.

Sample	Depth	δ 53Cr (‰)	2*SE	Concentration	52Cr	50Cr	spike ratio (.25 ideal)
200	0.8	1.115	0.109	33.28037	0.89	0.43	0.48
209	34.75	0.848	0.069	75.33588	0.95	0.14	0.15
215	49.9	0.633	0.114	28.0342	0.47	0.07	0.15
219	58.2	1.012	0.118	36.73122	0.96	0.13	0.14
225	69.45	1.216	0.179	28.467	0.44	0.37	0.84
236	100	1.24	0.29	34.35967	0.79	0.09	0.11
239	107.1	0.731	0.063	17.64795	0.95	0.11	0.12
244	126.4	0.927	0.081	16.81453	0.92	0.18	0.20
247	138.1	0.809	0.096	19.6913	0.46	0.1	0.22
249	146.7	0.624	0.077	44.83709	1.03	0.13	0.13

Table 2: Colours representing the two different formations and the standards used for ICP-MS, TIMS and IRMS data sets.

Tumbiana Formation	
Hardey Formation	
Standards (JDo-1 & JLs – 1)	

Table 3: 18ABAD01 ICP-MS data set for the trace, major and REE. Values that were below detection limits have been marked BDL.

24 -> 24 Mg [He]	27 -> 27 Al [He]	31 -> 47 P [O2]	43 -> 59 Ca [O2]	44 -> 60 Ca [O2]	45 -> 45 Sc [He]	47 -> 47 Ti [He]	49 -> 49 Ti [He]	51 -> 51 V [He]
4078.567666	4554.436196	308.6465111	98225.17753	114735.0733	3.528310755	64.09478798	69.79395012	24.44199835
8646.867657	10999.27801	288.2592336	20705.72178	24816.10651	3.513954802	232.9426446	247.6820438	36.217504
11262.20013	14592.6391	304.6872209	83411.24818	96289.52498	7.654280206	371.925332	380.7295632	68.86972315
16691.62558	8995.026292	169.6321933	130113.0236	151581.196	5.464560035	188.4289211	200.6004128	19.57122936
20380.39255	15909.54836	177.7765966	18480.53759	18705.22969	9.171902046	163.8208638	180.1029604	54.87840408
35926.93319	37535.25963	644.8912708	5238.631035	4773.987328	40.32905561	460.639959	485.0960666	96.31472481
12181.06728	11039.42195	166.985387	69030.54633	75538.92985	8.581788104	335.7249387	357.7211238	59.67916341
10418.32843	7742.676114	109.2387932	51888.97186	55186.9881	4.843514282	135.0932333	150.8244436	26.79337239
11358.49122	7703.619466	136.3418196	85467.37673	92362.72148	7.92625034	139.9112971	140.5516827	32.95232388
12599.83844	7474.818647	83.19243103	37355.95405	42167.99397	5.329641459	177.235171	192.6967497	31.21135805
6843.991275	8933.657417	469.812793	28895.0911	34409.91039	9.353101624	173.3957214	197.8215779	43.96266272
11485.63598	18225.50313	263.3887863	57805.19263	61943.717	17.18296518	278.6482902	320.9477412	67.24190493
11004.38201	18025.70455	292.7964033	57593.72855	57967.69394	16.1226854	512.8326722	569.1510886	94.10617874
20997.48041	34851.19491	397.6993301	4321.050102	4022.650961	25.32785958	610.7564952	644.8783015	169.8324255
17319.42575	30496.63042	499.4061854	19852.168	19310.56282	11.71748851	276.7765354	294.9518868	64.75226828
1591.921478	4563.775355	113.1547267	74988.86574	81124.73269	2.220839359	9.868394252	13.27189536	13.83174936
3499.715313	15240.67547	82.89836377	200966.0172	204832.195	17.53481554	37.838243	17.8736096	15.32554891
2679.749046	6440.291796	119.4674916	90423.43936	96467.12943	1.337814897	40.32489483	47.54404529	5.620443023
4852.169126	13005.10176	478.8463842	19695.10063	18521.62146	5.406577685	43.43856202	55.1214759	28.10242174
2293.830008	4947.14378	160.870121	141205.6315	153041.471	4.267850514	72.49318899	56.74413016	11.1486625
4355.630956	8025.048422	552.7103039	120845.0955	131268.6322	5.408488927	74.48364042	144.2579928	34.24308994
6221.480494	12557.93131	110.6918039	167896.2791	182705.8451	4.671496781	64.33343848	87.35896118	7.446258109
1361.144509	2238.842661	86.50961258	117468.7077	124351.6691	1.35459917	18.34815768	22.6673631	4.318726572
5166.346412	12274.04065	306.8399586	49466.28839	53861.44145	4.374499718	61.49262114	71.97109226	26.30714873

4049.301092	8703.43417	298.5724353	56933.09979	63046.79979	4.996184294	64.99751871	117.0647632	14.20253823
9996.187205	24196.47573	426.3869465	5375.725589	4667.806457	9.268231196	103.8038893	120.4195823	35.14946979
6623.606187	14735.10357	310.5558563	24133.05609	23278.55191	6.274222789	86.69687047	91.94207087	24.49294021
3644.364958	5582.51776	159.6865091	96208.32178	93862.11473	2.251364212	29.22663841	35.64406669	3.279653308
3112.569681	5180.185902	149.1121846	93545.39746	98439.08622	4.438597676	48.11953935	60.71033877	9.543784334
8684.994793	15935.35149	455.6093928	40480.70162	42571.91001	5.727756464	159.6228068	188.2869399	27.42873289
3229.357464	5070.383851	307.7202909	83383.30643	80765.1253	3.061641503	28.43386159	29.06389349	9.87780796
9854.871232	19675.60993	419.1373777	5942.967441	5892.822221	6.558729448	83.93083389	78.56669789	21.95652162
5617.904237	10924.378	240.8115395	27421.47504	26927.76795	4.051660722	48.48746853	50.05176296	14.44843398
19635.69602	30236.72325	352.8450902	20764.81967	18138.90932	6.837543501	190.4251186	223.0156237	31.06108676
4961.273562	6254.663075	214.8199796	88261.40014	90905.23051	3.077451977	71.95354487	80.38310779	17.85542663
5278.809276	4888.938977	120.3965597	136970.7817	141206.6471	2.997421674	66.94321997	78.31902051	11.13487958
4225.111017	4443.938796	302.0605282	129220.678	138553.4519	4.019924992	40.59627511	57.61674194	12.99831328
597.969395	652.5525642	26.62687311	17371.84599	16681.3775	0.259592291	8.561933908	9.81577461	1.741017713
-1987.340271	-805.3081175	-14.15158344	-9862.67933	-10400.67661	-0.480678738	-5.733492154	-4.262365971	-1.861830124
8476.375393	5854.345776	208.723666	78013.12712	68225.07016	2.413358142	35.6414303	39.79915763	10.09208451
9793.907143	6188.210581	184.0368699	107930.6234	115452.7602	1.047506744	36.68229579	34.86027893	6.235416547
6806.569336	2162.507163	31.87606811	33501.11948	31169.08182	1.882486593	15.78810717	15.32180932	5.542143695
1298.191863	926.6599576	13.72215756	198685.3932	208474.9299	2.492924415	5.502139105	6.479944534	1.772455894
5234.261807	5020.329141	201.5948367	96250.6146	99253.29288	2.024738402	72.07674484	85.97089217	13.24909231
4338.623911	4364.159124	529.9704077	99623.16991	102467.6051	1.861024442	48.22304638	53.43501372	12.26391408
9017.977835	8069.090355	424.0878535	93895.31598	90162.26637	3.285713976	109.6577183	124.2458277	24.29037518
6220.57374	4685.396268	255.4013122	81747.85156	85039.64713	2.84913117	99.87254916	65.90114979	13.82243868
5981.25668	6493.621851	210.1253172	76394.45852	80125.69363	2.383953403	133.0435238	147.1438331	19.87066896
3710.932982	4054.129961	262.6874993	107111.6178	107624.3105	1.901299773	79.41916901	96.68593623	12.26020162
8616.012068	7855.366382	138.460736	154018.1876	156154.8961	6.974052125	66.99028483	68.36547947	19.59424985
12452.04837	3950.622604	57.35236428	122847.2551	132659.388	1.476428629	54.98956298	56.53408326	14.73309258
20897.39792	6182.209163	74.75818223	155525.1575	161390.9701	1.400071671	111.3334488	125.0700995	14.143163

40429.00468	16222.29769	220.1265951	16520.09214	16891.1376	BDL	166.7118951	188.1809667	20.15440642
26920.58153	15001.27107	204.0140142	33793.23035	32259.01418	2.846464301	347.4590542	369.1122111	28.94471816
14387.10721	7145.60748	100.4525576	27068.61805	27080.70136	1.36498826	171.5027737	188.5260389	12.15745348
16029.46198	9392.965978	140.8895468	30538.27622	29411.65527	2.008501689	209.1833813	228.4477777	18.7171484
51335.09661	21988.23792	608.3623413	168705.0951	152917.0041	BDL	315.5428619	303.1834166	34.63470072
17850.71955	9581.754978	193.7041456	71985.39502	74929.7048	2.215579672	153.4739631	153.2970025	23.47565552
8026.595594	4112.697951	121.1990421	45650.88127	44501.63163	3.721992068	29.2404456	55.09500003	9.134920759
9793.91467	7445.374655	78.34265518	72863.0205	71823.19341	4.219079399	92.27300626	96.54560016	20.22416127
5245.571623	4771.642459	26.80047362	23619.4546	23763.22491	4.052550064	12.96743272	15.30166393	5.554473296
3190.26213	6590.945531	172.4476498	62110.33713	63776.52635	5.110342193	254.8331611	227.7884275	34.440574
2089.844435	5195.612573	34.85498617	104256.1609	105282.4827	5.393566381	34.40053328	39.10949188	9.918969133
4638.403682	15804.14671	107.2928223	66643.81601	67625.91776	9.466545023	56.52548818	64.22924878	12.68145317
2923.09881	11146.47179	841.3015348	5429.477274	5256.663144	7.341439941	40.90723662	40.34985922	21.73315818
352.8868951	1245.039345	5.230782434	63188.51324	67802.01252	0.312848018	2.85486811	2.42789428	0.418358928
979.420865	3445.340863	63.0333386	4643.546455	5037.982374	0.990317894	20.13043525	28.48138693	6.37001177
4114.999884	16109.12297	598.3217518	7528.624544	8502.343436	7.905619415	161.2043858	145.7966032	30.18822163
1152.251124	3251.622668	26.69820013	23083.00185	23132.17684	2.123773718	76.97960534	79.9063425	10.64359982
2630.099	6057.002993	27.31228634	132741.6752	137905.539	4.907750549	42.48777402	42.46012353	12.14928127
1512.75106	3905.926078	65.05739017	78017.03874	82887.23569	4.802587164	34.38767423	37.4641882	10.28352134
1751.954308	9784.052804	483.6003518	56863.24804	57559.77792	3.813614995	94.81406178	99.27771536	9.634143734
617.2815314	6918.02284	27.6683365	31386.05263	31204.27227	BDL	10.79202885	9.418699856	5.929952711
1402.213499	9.621987857	15.36345522	164995.9733	180677.432	BDL	BDL	BDL	1.002445523
1380.823905	8.43768325	13.85960815	173599.9969	174954.3063	BDL	BDL	0.111870712	1.131338024
48347.61625	24.65735612	62.96512269	100652.4237	112108.1142	BDL	BDL	0.329240783	2.134572727
54896.61475	20.08434928	48.80425198	120933.8449	128559.4415	BDL	BDL	0.268689509	2.408861036

52 -> 52 Cr [He]	53 -> 53 Cr [He]	55 -> 55 Mn [He]	56 -> 72 Fe [O2]	57 -> 73 Fe [O2]	59 -> 59 Co [He]	60 -> 60 Ni [He]	63 -> 63 Cu [He]	66 -> 66 Zn [He]
83.75717572	76.31996073	1911.509205	11118.94253	10927.1018	7.447866155	57.03982296	11.2570735	53.49645073
30.64440451	27.60961418	909.6239789	21912.2458	22113.40333	25.10678448	36.45152922	35.94017184	121.3816899
62.20331312	55.87155578	1745.194734	33655.75735	34271.35645	19.5917222	37.79605608	39.66134726	41.51608702
65.3620613	59.13321486	2926.830568	20227.45755	20681.23658	7.247360828	42.19078437	7.315903172	35.67982749
62.215816	56.04584717	1186.910266	29870.22695	30180.75504	22.37107241	58.13141118	40.82438451	131.6811233
358.9155608	319.3513693	1696.817982	78869.61959	81097.40228	57.97994422	220.9310851	114.1128855	458.3059334
76.58665106	68.64495737	2743.36718	25695.52815	26507.2857	15.25500196	47.25185591	38.88255278	49.01240168
48.45951336	42.18653499	1378.812476	16798.6108	17174.98479	6.532919275	31.8518182	14.95360713	23.55286772
50.22515278	45.89072051	1875.131285	15762.64901	15467.08861	9.181752829	51.63866485	17.10442095	11.69911526
41.10098238	36.69654922	610.300878	13312.48488	13264.32207	14.58793491	57.28306042	11.59024795	19.74498402
103.712547	93.47527246	496.6031672	20221.85884	20682.57165	10.66957293	36.69943362	45.29485559	308.3754227
166.4324671	150.8322913	2232.834761	44703.39351	45520.23166	22.44529765	95.20935673	89.86662416	201.1446357
185.8049809	162.2041555	2341.150494	45702.28192	47184.9292	33.69093714	265.639662	130.3237361	254.3836386
143.7577856	130.3598026	1885.384197	99726.0967	103866.1376	42.30970961	219.4657497	72.47495325	232.1203191
233.776636	207.4004148	1928.385649	104021.3374	104601.7108	35.76472079	865.4656574	178.5058717	755.6769237
14.808534	13.14345183	1121.794361	25766.41541	25389.59117	3.19580946	37.0943879	14.59440684	117.7326345
42.05844603	37.14553539	2839.698805	66877.22319	69125.7024	6.785485709	78.13195297	35.057213	231.5977758
13.07916207	11.18888798	1866.498119	13796.95673	13883.35916	5.006704489	85.33499506	24.57083399	222.3534908
385.2735877	355.7084249	791.0674457	45509.6132	46696.4265	48.24601819	471.8272523	39.72701025	319.871181
14.15163103	12.86027589	2517.968151	15902.07976	16176.25117	6.845486517	40.28115054	19.78890049	130.6019512
24.54669136	22.6085046	1843.957838	23918.7524	23787.43856	5.10163242	99.01005228	61.70533171	257.8528025
16.95360944	15.0301266	4894.52754	33532.73106	34309.48336	8.432286947	67.38335006	18.14748817	212.4775405
10.9715768	10.12534529	1492.306442	5962.950239	5981.680363	3.499429344	57.34577667	15.374755	124.706871
71.09876184	64.20705402	1354.157031	33834.15655	33158.46603	17.69059627	95.52109078	49.52754699	260.3700161
45.97438049	40.51678545	1716.510363	17751.55154	18050.44028	18.84201832	102.4087045	87.95911826	343.6092454

135.3868244	120.0416179	809.3897915	36412.53116	37736.44168	30.57470076	128.0096174	104.1808355	565.9236097
79.19835402	70.5189326	991.488818	29073.48879	29924.39001	24.57808933	69.0505186	203.4315252	527.6722484
9.885390232	8.698147162	2604.647017	6527.919708	6533.4066	3.482096762	24.22622812	7.719261209	144.9971228
24.15394708	21.97244122	1956.276733	10210.67537	10417.53886	6.30466433	27.84845785	18.78465997	96.10181534
88.69052543	79.30816136	1179.272331	27102.05149	27932.87629	20.94891259	106.3365855	83.49059273	396.4752792
23.44832761	20.98595503	1468.682946	9681.639333	10049.08747	4.139177498	27.66621604	26.71415959	132.0464306
102.2160552	92.85991473	690.9932142	28155.86757	28093.77739	20.02745836	112.4896439	121.8560985	502.520251
60.52047521	53.26310268	681.3776501	21008.34462	21369.35789	60.66647184	184.2411486	140.762135	303.4005073
130.1738539	120.8859736	1465.998793	27024.0877	27933.88504	56.68426069	177.224061	90.73089625	370.4610312
24.12278518	21.79455129	2278.205135	12902.0754	13063.41479	7.910296812	49.01379816	20.77500932	45.82741275
11.1262091	9.340705657	1983.257432	7866.245553	7953.643951	4.054748216	26.4557112	11.00875696	30.89179038
10.87379622	10.07983312	2050.338763	8794.640742	8670.82801	9.297360711	46.93549566	30.36378482	45.83259093
2.161188752	1.936576937	297.5665286	1247.171208	1238.85472	2.011436496	13.64696249	2.801197196	3.868512
-1.231075621	-1.126738883	-124.2912034	-1328.182111	-1379.572639	-0.752896988	-4.273542323	-1.136245256	-4.543942999
9.493837024	9.36520162	1248.041092	6436.494064	6633.371329	5.065840586	50.11147567	13.27907891	30.13655752
5.038847675	4.184246234	1696.450926	6003.78006	6177.1955	6.863261699	46.41457168	178.259598	130.3913446
2.873627499	2.419898731	326.4198685	3443.073786	3424.256274	1.895919249	25.07308093	5.537128416	8.591439762
3.546513791	3.089429278	2937.301004	4375.795995	4361.047941	0.551814113	9.064322382	2.843111099	13.38786741
17.68770521	16.04937876	2698.639266	9182.333028	9220.133638	4.990201592	48.0878765	18.91728325	76.32201018
13.86694154	12.40476922	2310.89656	7842.113203	8038.753061	7.877577322	45.99406358	24.13616461	45.89472077
22.79917984	19.47741885	1627.027064	15368.93957	15694.14718	9.140088393	43.93840937	32.3371762	33.60605398
13.15216043	11.01256939	1841.6144	7830.84571	7954.201103	3.937631298	15.76548207	28.627377	BDL
18.796605	16.52410401	1726.369515	12979.35341	13216.59704	6.677185904	31.78092838	20.85334435	45.53953999
13.27641953	11.73532322	1532.08245	7814.83596	7761.5281	4.227785583	16.73281356	40.75339865	20.86200362
18.55724709	16.5326198	2289.597146	14815.43136	14628.93372	6.504698869	19.27419989	45.85582016	20.43813946
143.4879512	131.3552471	866.5161177	7730.905315	7917.837772	5.285687701	343.5458516	5.20742534	15.55342745
176.7567924	160.1685643	1385.048505	12675.92269	12856.88233	8.585386165	1328.682004	7.206882898	BDL
517.7307297	448.9923843	1171.01032	33785.66646	33883.18098	29.70012758	237.454299	10.60502657	BDL

421.5710888	369.6004694	1091.875518	35106.18401	35525.03415	21.64425674	119.800447	11.95096371	34.94659332
220.5525957	198.644364	605.1435755	13561.17305	13793.87179	10.4784119	74.65998677	6.355363681	BDL
275.2164709	248.3782081	706.9865116	22266.66642	22551.96986	14.09795828	98.53174552	9.876160604	BDL
709.7678368	635.2287896	2392.156773	33995.56312	34677.4372	34.88800229	241.4232203	18.84954913	BDL
276.9800925	247.0710097	1021.988139	28263.34508	28755.17769	14.4586088	101.2752817	13.5651644	BDL
111.9305084	99.60653385	422.1705392	6709.295181	6765.067123	5.383202821	42.93539027	2.105000843	BDL
153.6159832	137.6860812	1098.353565	17623.28011	17645.14014	10.21934666	56.09183198	8.115965748	13.15848032
103.1593227	92.28235026	788.1722705	7569.547537	7656.918	3.451990764	17.86880688	3.490309486	BDL
44.14121018	39.4848891	1283.781267	15999.05027	16122.52222	8.315443331	21.95107415	21.5584715	16.71662536
19.11797936	16.76086433	2941.547392	12593.79333	12705.5274	3.08219491	5.903829194	9.735529707	BDL
48.3959524	42.44211081	2109.544506	21543.47685	21431.00988	9.295283066	24.2910776	40.30446684	347.0307127
23.90898018	20.69574954	542.1755306	19283.42437	19365.66249	7.464019481	14.50382341	43.84221062	53.49723325
3.880931419	3.199427354	1266.473607	5346.39964	5408.836627	0.508616774	1.004723545	0.716149067	BDL
34.77874272	31.95645429	489.5658107	36329.33172	36779.73796	2.79620053	5.983177383	2.96068541	BDL
44.09997749	40.34840454	581.3164921	28124.89488	28136.60598	13.96432089	24.19715478	72.90629632	BDL
21.5468906	19.88284516	442.8937005	14887.75991	14870.35871	7.283282319	11.94145036	7.229512589	5.743257242
32.95244807	29.42442531	1724.934057	23908.80408	25049.7812	5.229374794	13.97389794	10.6220694	60.44330628
13.42838264	12.225852	2191.21925	12339.02828	12359.90438	3.336670993	8.098176849	5.948349726	BDL
29.65156681	26.33942462	2230.709215	16380.76419	16399.262	4.586469277	11.4075126	11.26855519	38.45650804
45.84494986	41.88598501	1225.452536	55353.64111	55456.00005	4.237625081	11.96434167	13.75008928	BDL
0.387038512	0.260077089	9.18880448	28.3274541	18.05657956	0.046566153	#VALUE!	BDL	20.23602078
0.592604503	0.525015415	10.93033725	30.73405331	17.68811336	0.033885808	0.232187911	BDL	BDL
3.951429036	3.515996239	30.49665344	83.50537874	78.36306403	0.12340496	1.846656991	0.173743636	8.837614349
4.810634452	4.17713784	38.0285024	84.84566161	78.74597751	0.143890326	2.001463669	BDL	13.90760335

71 -> 71 Ga [He]	85 -> 85 Rb [He]	88 -> 88 Sr [He]	89 -> 89 Y [He]	90 -> 90 Zr [He]	93 -> 93 Nb [He]	95 -> 95 Mo [He]	98 -> 98 Mo [He]	111 -> 111 Cd [He]

1.918093235	1.953701715	146.5974553	8.472815393	2.078983891	BDL	1.079463976	1.016064681	2.634956902
3.300582636	10.6910192	54.69649968	9.342964728	3.952117011	BDL	0.144184575	0.12951096	6.599004165
5.601446086	3.228327542	134.3849004	13.23410418	6.278181599	BDL	BDL	BDL	3.106947948
2.175776772	1.307886225	309.6733672	24.6609962	2.655447861	BDL	BDL	BDL	0.408042395
4.242521309	1.953457616	63.30966596	7.767514667	0.672983915	BDL	BDL	BDL	1.244901177
8.497319188	27.31528815	170.2843834	30.64268759	3.012815813	BDL	BDL	BDL	4.842107763
5.161551174	1.685959396	146.5192093	9.664763347	4.120842518	BDL	BDL	BDL	1.537278355
2.299995524	1.732386408	98.73506641	6.901798157	1.797403911	BDL	BDL	BDL	0.12593472
2.401341971	1.147976602	170.9963719	11.94869309	1.672606402	BDL	BDL	BDL	0.677347386
1.830988905	2.620579901	83.46935531	4.257245507	1.965123487	BDL	BDL	BDL	2.725183186
3.429707433	4.998373489	61.35252796	16.0543493	1.751824242	BDL	1.17959299	BDL	8.539816698
6.432372666	12.05529632	148.8912538	19.76900623	4.969520171	BDL	2.329960747	2.494388101	2.393370194
9.124876393	10.11932461	107.3418319	17.15051708	9.217754926	BDL	BDL	BDL	6.577527334
14.13967883	12.8132104	77.91787594	15.44683526	7.185451273	BDL	BDL	BDL	8.924343853
9.010982924	9.032478046	54.8846508	11.74343227	3.308486594	BDL	BDL	0.466315128	17.65266984
1.538670614	11.66920685	209.4122513	5.086629647	0.736477316	BDL	BDL	BDL	0.975084032
2.771543073	4.73118824	307.4565687	14.43472053	3.577694089	BDL	BDL	BDL	1.199082679
3.316819382	26.65870588	152.3382004	43.76379018	4.88662554	BDL	BDL	BDL	6.473291301
4.193247827	18.94336135	29.80483271	38.10487849	4.921238506	BDL	BDL	BDL	1.47308095
1.588327541	9.623865176	190.6089049	18.7743638	3.407371023	BDL	BDL	BDL	1.912705621
2.946118716	12.76515855	216.526449	22.87629376	5.458535402	BDL	BDL	BDL	6.023145968
4.224869901	15.375991	313.6468768	86.87545931	9.886981278	BDL	BDL	BDL	1.762792357
0.845943577	7.058669987	88.69163659	6.283930882	2.301675479	BDL	BDL	BDL	1.771754845
4.68340157	19.56515928	78.59275136	15.34508712	3.16831277	BDL	0.459599107	0.413060859	3.208248321
3.610035483	22.09120472	96.96046253	21.63082136	1.911596734	BDL	BDL	BDL	4.72074044
4.672286588	90.13462658	58.28343847	31.42118319	4.077251773	BDL	BDL	BDL	9.320234396
4.987855228	35.40842556	57.46575631	15.07547013	3.218218622	BDL	BDL	BDL	2.675994983
3.378885661	25.64196634	177.6658965	20.94823531	7.170163949	BDL	0.618618547	0.683346937	11.47449191

1.445855064	13.2201296	119.821611	7.770946989	4.366818673	BDL	BDL	BDL	1.566413603
4.797413316	47.90204545	116.7177253	13.73942517	7.811508691	BDL	BDL	BDL	8.949996645
1.180671917	13.59495877	93.56867009	10.58227043	1.182861052	BDL	BDL	BDL	0.569610877
4.660402526	61.17528285	57.2145755	12.31289793	3.552463147	BDL	BDL	BDL	4.905937673
3.105592027	21.62265039	58.81400378	10.75531529	2.289368023	BDL	BDL	BDL	3.261972469
5.848281224	151.0503371	75.60685105	18.90162003	8.627418527	BDL	BDL	0.84618005	61.091198
2.266434661	16.35203286	89.82962896	7.065919496	2.578722528	BDL	BDL	BDL	16.84186914
1.307518498	39.16876123	152.8046255	7.032726502	2.308370769	BDL	BDL	BDL	1.40479992
1.178554361	20.20257615	142.9844691	9.568042725	2.584801755	BDL	BDL	BDL	6.832057301
0.173707533	4.724811113	22.77389869	0.89730718	0.303159703	BDL	BDL	BDL	1.647278728
-0.166145921	-3.838452276	-17.03097856	-0.922126855	-0.2081758	BDL	BDL	BDL	-0.175058911
1.619888187	66.17551051	173.5826919	10.95780898	6.918613489	BDL	BDL	BDL	7.961709451
2.411073891	63.0566636	207.6861051	13.81864322	10.18511748	BDL	BDL	BDL	16.49186486
0.526026074	8.453348756	54.54957447	1.482801103	0.568130298	BDL	BDL	BDL	1.034048623
0.29803681	2.272088088	147.5469922	6.177167598	0.3888849	BDL	BDL	BDL	0.290362648
1.430636745	32.03472255	97.58697482	6.645650714	1.399652368	BDL	1.024822628	0.974257901	3.682151982
1.204352667	20.81020465	136.065874	8.186035994	1.99695927	BDL	BDL	BDL	5.076308229
2.108028923	32.35825732	139.3137715	11.7249868	1.835735363	BDL	BDL	BDL	6.229919192
1.402360621	42.02538257	92.38110878	5.494041711	3.628945355	BDL	BDL	BDL	2.6482865
1.776378299	52.28647507	122.8326902	3.991982935	4.619059717	BDL	BDL	BDL	2.205024016
1.298857349	34.3063285	156.2046835	6.481716403	2.55911587	BDL	1.388201782	1.255214065	3.527344183
1.500177028	41.96992338	173.8665099	8.986364878	0.854829596	BDL	BDL	BDL	1.888486119
1.379022945	3.680255877	277.8213287	4.133075697	0.711603027	BDL	BDL	BDL	22.79847698
1.910067809	10.44327368	179.9808491	10.76344947	2.115151097	BDL	BDL	BDL	0.765237023
2.743653667	16.01381669	152.3798254	11.3997764	#VALUE!	BDL	BDL	BDL	192.2516871
3.377506701	11.20913956	116.6939899	15.26162054	1.660903211	BDL	BDL	BDL	0.725580023
1.389644009	3.954101671	134.3098269	7.55513724	2.36557348	BDL	BDL	BDL	0.04788773
1.835372511	6.475901102	131.8868534	7.617625468	3.509573488	BDL	BDL	BDL	0.019844834

3.095688521	31.29216025	584.4212975	25.86210052	BDL	BDL	BDL	BDL	0.501950289
1.62330993	8.367398217	167.3190458	10.78497888	1.489128338	BDL	BDL	BDL	6.215943446
0.960550095	1.855544676	91.08421804	5.749577957	0.859701337	BDL	BDL	BDL	0.40289286
1.855955643	3.283485864	94.73910398	9.562540403	2.394096269	BDL	BDL	BDL	0.01879797
0.833893784	1.831415804	22.07119412	6.379674414	#VALUE!	BDL	BDL	BDL	3.056997823
2.82657081	6.305303156	57.3312503	9.737031249	4.85887582	BDL	BDL	BDL	0.226559147
1.205638525	3.38629531	74.25542873	13.03458515	0.727499391	BDL	BDL	BDL	8.067841671
2.446393962	49.24842472	127.2703723	23.05569313	3.218468517	BDL	BDL	BDL	2.790277481
2.197417077	29.50433124	54.03415376	25.68684379	#VALUE!	BDL	BDL	BDL	0.164017669
0.330817503	0.829055014	46.15743238	3.771160654	0.299676399	BDL	BDL	BDL	0.010874715
1.080688188	7.311022162	18.10937761	4.062349046	2.438530189	BDL	BDL	BDL	0.147953365
2.964950919	123.1398018	60.22171341	14.21450708	8.761649196	BDL	BDL	BDL	29.14684364
0.992044706	3.49447827	32.08885531	3.210093635	1.853655163	BDL	BDL	BDL	0.016598631
1.078363002	4.888154847	165.6563311	7.379951032	1.049478954	BDL	BDL	BDL	0.03489557
0.701916526	9.527447695	68.32596087	14.77814849	0.814852865	BDL	BDL	BDL	6.802980133
2.828727292	37.22825066	89.48072575	14.3655593	5.832774729	BDL	BDL	BDL	0.069980214
1.481449618	29.56846591	38.82248745	3.116822162	BDL	BDL	BDL	BDL	0.917131274
BDL	0.020032976	174.3004632	0.112878642	BDL	BDL	BDL	BDL	0.255219448
BDL	0.014956537	184.0066423	0.122503099	BDL	BDL	BDL	BDL	0.08862897
0.052666546	0.031822759	91.30287979	6.263816626	BDL	BDL	BDL	BDL	0.31091542
0.069798591	0.017450486	108.7518935	7.489870065	BDL	BDL	0.162605836	0.162361446	0.337463102

133 -> 133 Cs [He]	137 -> 137 Ba [He]	139 -> 139 La [He]	140 -> 140 Ce [He]	141 -> 141 Pr [He]	146 -> 146 Nd [He]	147 -> 147 Sm [He]	153 -> 153 Eu [He]
0.368274123	14.66945704	12.41789428	20.08146102	2.143043872	7.752992592	1.421042154	0.27223139
0.182617326	152.4117364	16.30747177	25.81189739	2.835345627	10.49562727	1.633606261	0.376757262
0.568470139	37.10443351	20.24040256	31.0382393	3.353086736	12.39785757	2.302520332	0.524911804
1.4327008	24.15042733	11.35778594	22.07235703	2.806275649	11.96042552	2.753792545	0.556255559
1.48072536	22.41086308	8.576188303	14.12786532	1.484478983	5.589479356	1.047520215	0.273287379
6.192533208	383.6526534	42.63691517	82.007354	9.642830626	34.48288827	6.410514373	1.195236397
1.813423792	21.77378992	9.329112468	15.65988033	1.779375293	6.782829878	1.344321535	0.337424939
0.648020405	19.26063204	7.620003453	13.75783769	1.417738651	5.342013266	1.026032969	0.252382451
2.314891756	19.31857906	8.422401128	11.83918817	1.315400736	5.372481387	1.289818586	0.36321776
1.338995184	92.56409203	6.436844326	10.38430622	1.008104574	3.634732952	0.583541603	0.173514085
0.686363635	59.98632504	38.2088062	61.8968368	6.099430447	20.09176668	3.157652421	0.61070523
2.00187503	101.6049531	43.18283129	77.9283885	8.443840081	30.3337073	4.674734685	0.861734427
1.042075965	50.91944674	55.97840588	94.91936405	9.679719074	32.81612668	4.23055497	0.741918783
4.688297655	47.88726024	25.69923695	46.07706747	4.943023719	18.69444759	3.133986495	0.670965625
2.152471121	31.32041866	25.98832341	47.53891436	5.044377433	18.83364763	2.863986222	0.555592795
16.08736214	251.53208	6.155028637	12.17867996	1.486364511	6.467712505	1.602852186	0.422810013
10.82303914	17.3722868	24.41195647	45.7093279	5.088746694	18.54363727	3.652851538	1.058045503
1.713210423	37.86967545	17.84054226	41.85746712	6.226148999	33.72569934	10.13481112	2.449795886
0.880650283	31.84839744	26.78456584	58.37622553	7.773828723	34.12736918	8.220958415	1.678171389
1.558035763	20.96359941	12.30208299	25.00646387	3.128726676	13.63246975	3.063540674	0.738007743
0.681243785	17.26150803	10.12465089	22.75097262	3.16570897	14.94867348	3.573329058	0.805010992
1.133925233	38.69348486	47.82426522	98.77108894	14.5518945	63.21843256	16.61980672	3.789263396
0.338789751	13.22431204	10.85069413	20.13525836	2.265929684	8.334963656	1.388832005	0.307535158
1.34209014	37.86348321	48.7889803	90.64141037	10.58269128	37.4777172	6.05863473	1.016713835
1.500619482	42.62813185	55.60163275	111.5851857	13.0758324	48.29701548	8.318237208	1.685223694

7.280935997	153.0907388	60.81006637	125.3284848	13.97244956	48.72994223	8.489257165	1.36642621
1.560159088	70.59107569	80.91815675	147.9118154	16.02198048	54.60932395	7.263784807	1.324692176
3.311831381	49.22052097	113.1107644	164.314306	18.46862431	60.58024566	6.68509269	0.76199585
0.547678429	39.53057754	18.33456636	28.74652401	2.610378064	8.402259903	1.395219887	0.341040797
2.837320966	106.0091995	108.0737177	142.3698762	11.95283378	34.01012003	3.75171993	0.787657748
0.235400937	38.38418547	15.73463578	28.68630884	3.144909699	11.65028758	2.213060203	0.472249324
4.182627666	135.8797159	98.28811244	163.1949499	14.6883188	39.93254659	3.420644199	0.555679173
1.062442752	61.17760036	69.99397539	109.1097747	10.35187553	30.40494888	2.899744206	0.47533354
7.056378181	296.834784	102.475409	171.8798468	15.95936134	46.09003027	4.637959859	0.765829079
0.904305939	35.14011259	12.03715709	22.82027699	2.421913842	8.208530084	1.221966208	0.321203183
1.923168344	48.29195265	18.43524338	29.3693413	2.654590224	8.076858923	1.317772565	0.28111657
2.111120758	38.46982005	12.70909008	22.58378742	2.344488094	9.058104754	1.620585008	0.446001301
0.348401563	7.135585473	1.73364686	2.971098513	0.312263923	1.033486807	0.186780411	0.03889386
-0.310904857	-3.824465823	-0.786322267	-1.54874465	-0.191105818	-0.80376773	-0.152618145	-0.03066482
10.21274611	85.80710847	25.20551503	41.11365741	4.11818184	15.39792809	2.376093819	0.334358012
13.19033517	98.91921004	70.65833658	100.5906118	9.925734429	33.33380947	3.992313591	0.352051618
1.926676725	10.14804702	1.617229453	2.560631787	0.29851371	0.936942483	0.221928742	0.09679505
0.22213284	7.141340619	5.199140295	9.230083939	0.988280674	3.714859318	0.70839048	0.166791123
2.241563762	48.11019041	9.202161303	16.38711477	1.775108164	6.325569987	1.045518259	0.248009081
1.718572548	42.9057562	10.4910976	19.37432366	2.161485574	8.677710036	1.690278648	0.407411524
1.818970541	46.25096179	7.88967615	14.30738934	1.857818756	8.014348113	1.853308807	0.504590029
3.204079745	44.97654837	6.396670943	10.54051662	1.154936287	4.543082441	0.986620051	0.249775201
3.148490407	63.16768911	7.288606233	13.19289586	1.391459314	4.948722276	0.704430182	0.16602688
3.630334222	44.10783635	9.156217396	17.7852579	2.008046765	7.114542369	1.265510071	0.313586534
2.585506256	57.3503058	4.058500477	7.866883069	1.039767849	4.612624787	1.215938133	0.364258821
11.00282964	26.46328674	3.06320189	5.689274135	0.717989514	2.99159726	0.690976375	0.187806994
14.03210508	56.08508551	8.029615171	16.65365713	2.084841721	8.609719043	1.791743642	0.432379516
39.92752431	74.38104875	13.33339421	25.74844106	3.216494822	13.83046906	2.692302667	0.656537214

15.81208769	120.5000177	18.40518023	36.74770924	4.519119503	19.511367	3.95856767	0.60659358
11.70177469	46.9794462	7.593270771	16.26663845	2.165775838	9.772869002	2.0977557	0.324822168
17.60215062	63.12205853	7.191946944	15.08601125	1.929413114	8.507988113	1.65353927	0.345556648
107.1654888	229.1782461	30.53064164	58.42381644	7.519113535	32.60410745	6.302249408	1.156064859
22.28160253	55.68667712	11.76076096	21.19119312	2.434115719	10.14923331	1.98943238	0.429712956
7.053167772	17.70441003	7.191738736	11.58073448	1.392242917	5.574434443	1.071037096	0.185567167
2.761530123	38.32112013	7.766277105	14.43464401	1.793213094	7.573250112	1.600183655	0.357882864
1.153614575	16.24720125	6.561792584	12.14882033	1.51744076	5.352240435	1.139527143	0.323125383
1.004732211	37.5561712	10.53932653	20.39253973	2.482551611	9.876885733	1.87786669	0.433609913
0.490458928	30.13487878	8.807483045	15.51028818	1.846294289	7.134421983	1.643762845	0.407412697
4.19124725	332.0180966	27.64880925	52.42094673	6.39616366	24.7522352	4.752312407	1.035700234
5.201523408	155.9741052	17.16058424	33.39341015	4.529312877	19.25134276	4.510611799	1.042792733
0.04257972	5.495173427	2.957833233	5.348939547	0.593238271	2.405360468	0.534825397	0.170730708
0.198986245	39.82829768	6.309807391	10.8800691	1.296093064	4.633062504	0.9167484	0.189510518
14.46498534	278.8024451	22.60842976	40.20092303	4.575858224	16.82785041	3.375006534	0.838468881
0.121403866	23.01615193	6.456760633	10.65518345	1.116918316	3.954190108	0.735303706	0.161179331
0.336562058	40.32679169	6.970263154	12.01073911	1.445615277	5.790487419	1.196454571	0.318231971
1.699393179	37.15152187	6.700647414	12.35197295	1.476522513	6.550068862	1.428706956	0.469214079
5.747417765	143.9209908	31.30292742	54.1328836	5.705304802	19.65467485	3.520840455	0.839857269
2.259859294	117.4111827	11.30814264	18.7628111	1.978607935	6.641152178	0.970779414	0.207368999
BDL	242.6535946	0.050863344	0.085572624	0.011607955	0.040192445	0.012899102	0.02062625
BDL	164.0879945	0.05596495	0.10573283	0.012205808	0.054395746	0.014844641	0.013644038
BDL	4.941272029	5.039809895	1.330927835	0.661273329	2.620624983	0.448326161	0.102992531
BDL	6.758942008	6.038189194	1.547233439	0.770109132	3.061571598	0.543717765	0.113721258

157 -> 157 Gd [He]	157 -> 173 Gd [O2]	159 -> 159 Tb [He]	159 -> 175 Tb [O2]	163 -> 163 Dy [He]	163 -> 179 Dy [O2]	165 -> 165 Ho [He]	165 -> 181 Ho [O2]
1.471289092	1.488866969	0.208655176	0.204880613	1.33678284	1.286683187	0.290497749	0.308499062
1.710552	1.766528447	0.266811655	0.255669066	1.538531708	1.609017505	0.3355961	0.341362123
2.4300667	2.449772915	0.367600739	0.359185799	2.313437796	2.355132798	0.474481815	0.497988593
3.4163514	3.405500535	0.590025779	0.564548202	3.767744947	3.919602075	0.865492376	0.884417465
1.145585546	1.17993619	0.207768945	0.188910224	1.274063705	1.261060929	0.282289776	0.277916165
6.623290596	6.590492455	1.047050343	0.968895877	5.960362303	5.490762285	1.121965995	1.174760809
1.705236485	1.668219945	0.276009565	0.257754548	1.641880955	1.622433173	0.356180546	0.340823845
1.136704459	1.203021455	0.195804424	0.184521976	1.134661578	1.19030692	0.240434688	0.258140061
1.607119944	1.690035203	0.285436631	0.284492884	1.946458506	2.106302597	0.405359796	0.457639377
0.700970764	0.679878552	0.098772786	0.094667268	0.716518679	0.656326134	0.172430424	0.150669103
3.171616549	3.702020615	0.488788451	0.564270209	2.867578256	3.434546055	0.606424734	0.722585608
4.57533979	4.623333877	0.645647753	0.630093235	3.677075231	3.773956792	0.758299651	0.787804025
3.925110578	3.604330945	0.525311306	0.516882683	3.162394128	3.070859338	0.661737416	0.622509608
3.23297856	3.125701674	0.438440912	0.429225404	2.534814886	2.507449178	0.514612999	0.5446978
2.852659219	2.609047119	0.391383545	0.362730241	2.021196431	2.000947739	0.436291403	0.438363485
1.417356708	1.414694382	0.193304786	0.188622324	1.005272174	1.038486989	0.193615185	0.195752676
3.858910827	3.726852105	0.54602062	0.52647723	3.001741429	2.993670832	0.55688718	0.593769328
11.88784585	12.09430697	1.645376244	1.540039019	8.869499718	8.786098884	1.583780104	1.69042163
9.554918815	10.58431308	1.514897228	1.621366644	9.375242651	9.736924123	1.774794441	1.91310918
3.666904402	3.648319822	0.52712062	0.526418034	3.127954595	3.292862056	0.684853656	0.694415268
4.311374458	4.493099954	0.620219485	0.629180812	4.026110348	3.870028627	0.706555037	0.795151554
20.34736303	20.23882734	3.137842421	3.071241781	17.54163956	18.16595209	3.360559432	3.384017625
1.336047769	1.427937043	0.16688126	0.179526712	0.971774143	1.053749896	0.22661699	0.234707994
5.343440316	5.331400837	0.687375621	0.651916806	3.435750677	3.460830069	0.650032166	0.606049282
7.307740243	7.20804973	0.904163912	0.908156188	4.614921171	4.552820828	0.823836835	0.851698152

8.335504533	7.906999445	1.182427938	1.061845062	6.033911989	6.260163158	1.141038179	1.227715534
5.80747086	5.420193644	0.648506331	0.597385119	3.009803234	3.002116565	0.569388648	0.577856379
5.447522288	4.962332215	0.577354464	0.533438332	3.032492108	3.036421072	0.657470754	0.660902015
1.633040124	1.49787369	0.25215346	0.213628153	1.340770592	1.413456638	0.305459089	0.318922354
3.964288984	3.610557529	0.493438714	0.457377313	2.608747832	2.763504966	0.509561022	0.537999414
2.182017403	2.550018204	0.335999807	0.359830957	1.883881361	2.114232123	0.394669125	0.465236865
3.453921883	3.127418859	0.427988291	0.392694456	2.194546149	2.183015935	0.448327777	0.45640683
2.917681714	2.642458138	0.338504183	0.338022456	1.834363372	1.926880646	0.386502708	0.413589703
4.715650027	4.228059257	0.574783578	0.56660422	3.079221852	3.354399169	0.655932753	0.738282383
1.49947153	1.496606246	0.204639439	0.211756527	1.177888799	1.314300798	0.278019139	0.290977106
1.368008554	1.337403479	0.194231289	0.180694484	1.163655916	1.235312671	0.255097713	0.267841845
2.020491221	1.94051118	0.262944633	0.305699164	1.592472297	1.751336941	0.343064821	0.360761547
0.187703148	0.177181482	0.027441155	0.026944149	0.155583722	0.156469112	0.028777805	0.037817201
-0.156652111	-0.15452138	-0.023729582	-0.023891707	-0.159319559	-0.1455462	-0.03383099	-0.031017239
2.353296245	2.076789113	0.291771068	0.314071599	1.771610011	1.936634087	0.397340672	0.388780024
3.420810823	3.538897506	0.437742453	0.428676651	2.009582122	2.181213219	0.50170804	0.525454112
0.348995845	0.325300206	0.056765916	0.060603022	0.261266701	0.273503986	0.076404155	0.078769618
0.856520758	0.880989872	0.142201017	0.134385777	0.884602516	0.898555243	0.203002129	0.221659304
1.261431785	1.376148347	0.187656241	0.205444857	1.204499523	1.229572181	0.266629233	0.255622326
1.927207951	1.913477303	0.269622904	0.251389469	1.512240722	1.484535371	0.295376233	0.292595981
2.199189694	2.019052553	0.335796796	0.315546454	2.006621423	1.914879854	0.434345506	0.418881905
1.082988714	1.07798617	0.177499763	0.190702968	0.916977203	1.011911848	0.21820427	0.262747964
0.931101129	0.87300178	0.116968445	0.114723561	0.758085973	0.756451087	0.139639614	0.148413597
1.597764397	1.61158913	0.220773612	0.231463644	1.224822931	1.338258169	0.256262854	0.274461193
1.547809657	1.520665735	0.260140102	0.240055097	1.567607688	1.676115308	0.316625745	0.390993488
0.787077579	0.771381488	0.118295058	0.108058252	0.571176998	0.646128117	0.135753683	0.143678326
1.973258379	2.05017561	0.256923789	0.310691428	1.805378483	1.979682571	0.383331379	0.412167031
2.793266633	2.567310441	0.387030115	0.298470568	1.998391189	1.957693726	0.339455148	0.411877522

3.692875438	3.808676869	0.438470662	0.436138286	2.510801198	2.554043797	0.54324861	0.506439978
1.755438829	1.743344084	0.217355978	0.219183655	1.241776394	1.331278446	0.246791613	0.256685642
1.583195043	1.613599192	0.198383969	0.193614268	1.269198845	1.248082957	0.258035994	0.283926022
5.631139895	6.519311308	0.739627261	0.760125353	4.054784876	4.508552236	0.930028839	1.095264524
2.24333068	2.058055277	0.315337384	0.293561871	1.863842842	1.751952633	0.360950823	0.352587835
1.143355724	1.191812724	0.152263693	0.164891486	0.910837581	0.926685281	0.175966506	0.179972705
1.710171103	1.851776226	0.246329804	0.26566679	1.529992147	1.651329785	0.340777108	0.358021898
1.196496337	1.271981033	0.221996321	0.249744795	1.065964189	1.064964107	0.268438824	0.300734898
1.99402703	1.992735534	0.302932245	0.331234909	1.812215025	1.903419127	0.39000931	0.416850912
1.863475589	1.899214134	0.299002888	0.346685354	2.032118933	2.096692537	0.521835065	0.550698517
4.943114858	5.084262169	0.636349751	0.718653821	3.552345367	3.951748456	0.846135243	0.94814606
5.158166691	4.923311065	0.76615478	0.794146161	3.888526584	4.221126524	0.895550991	0.999870727
0.654793279	0.729851474	0.109457972	0.123163703	0.589731004	0.607842155	0.131122613	0.139952542
1.006809675	0.946722503	0.144024447	0.187411984	0.677057373	0.811170825	0.173438407	0.205466128
3.439526813	3.126002967	0.399613232	0.536677468	2.360540225	2.624037238	0.570192321	0.755996708
0.686302889	0.708757555	0.101281085	0.112484483	0.563022072	0.583084794	0.125476343	0.137552967
1.538940275	1.56283141	0.222107621	0.247297337	1.2050132	1.244504069	0.267233243	0.293844121
1.978842711	2.096965403	0.338922426	0.387708145	2.256729786	2.384855192	0.517886084	0.561038084
4.066836514	3.768808807	0.509507093	0.606050745	2.620301726	2.864621736	0.513835765	0.604479286
1.068600128	0.990385702	0.127371636	0.253276771	0.661486377	0.81965081	0.171831537	0.262075562
0.00794129	0.017800884	BDL	0.010063981	0.012126637	0.018867229	BDL	0.011365717
0.013126025	0.017748417	0.002383381	0.005219252	0.012571271	0.014196434	BDL	0.006045232
0.530060218	0.506361394	0.07711236	0.075153328	0.41184719	0.456118549	0.101685969	0.099610566
0.661689421	0.662275646	0.095647752	0.088191803	0.546331939	0.53510546	0.117251357	0.12670622

166 -> 182 Er [O2]	169 -> 169 Tm [He]	169 -> 185 Tm [O2]	172 -> 172 Yb [He]	172 -> 188 Yb [O2]	175 -> 175 Lu [He]	175 -> 191 Lu [O2]	178 -> 178 Hf [He]
0.982137662	0.138797706	0.14161227	1.038126869	0.972366622	0.174495407	0.17579676	BDL
1.028670158	0.142306103	0.141063454	0.944004581	0.88534847	0.141835578	0.149357974	BDL
1.440013626	0.212299109	0.200350632	1.453850956	1.477500259	0.218223511	0.204418491	BDL
2.639121337	0.377188553	0.384680078	2.540946481	2.581847168	0.393004764	0.402661545	BDL
0.855670734	0.122789034	0.123603759	0.823136786	0.793402859	0.129887424	0.11853431	BDL
3.250247282	0.409260762	0.475183401	2.573548158	2.463705882	0.42475698	0.379907958	BDL
0.952308829	0.134606381	0.143262648	1.020558876	0.894472706	0.161230143	0.149649591	BDL
0.774586254	0.106307173	0.117766537	0.70656661	0.750560183	0.109606036	0.127602289	BDL
1.596384642	0.197868326	0.212945789	1.339516138	1.512399095	0.240084582	0.241680283	BDL
0.447452865	0.069253547	0.066533251	0.455350627	0.361078616	0.07682494	0.0733936	BDL
2.192169698	0.247373945	0.316262908	1.711925017	1.94221889	0.254902371	0.290231829	BDL
2.244262308	0.281474464	0.286821972	1.850945589	1.923268997	0.280849568	0.274543087	BDL
1.894825399	0.253396353	0.241959087	1.703017968	1.628166239	0.246702217	0.25073121	BDL
1.53652323	0.191115844	0.213172812	1.275418924	1.274016597	0.181287349	0.181899368	BDL
1.207119447	0.178262058	0.191351622	1.084506764	0.997344102	0.169864639	0.184090537	BDL
0.500824077	0.058546827	0.064158983	0.410713667	0.407898025	0.072570782	0.06044545	BDL
1.562176221	0.197322693	0.203670247	1.319093867	1.267852182	0.189812776	0.214683168	BDL
4.212302331	0.500585299	0.545539589	3.199581353	3.045024616	0.431622423	0.441754465	BDL
4.8267088	0.558830051	0.564696866	3.037016462	3.048904127	0.43202765	0.448729604	BDL
1.996652879	0.237378868	0.261801463	1.699691325	1.594639898	0.289238411	0.296522812	BDL
2.197946902	0.296512144	0.300405704	1.887602789	1.785346302	0.304409867	0.28695905	BDL
8.270603995	0.984379969	0.955283152	5.241526527	5.156408922	0.735624738	0.759725494	0.311496715
0.666098889	0.090442514	0.099369331	0.704525975	0.6896444	0.10801826	0.112686122	BDL
1.623220021	0.184177202	0.193415151	1.089653546	1.203716615	0.144480355	0.167849704	BDL
1.957339006	0.233287778	0.243661108	1.362640041	1.299207719	0.205278972	0.266770538	BDL

3.020828881	0.378407746	0.370856528	2.314488246	2.045785192	0.352329428	0.288277042	BDL
1.546512202	0.191656178	0.203718641	1.306314674	1.08061177	0.182727216	0.187218958	BDL
1.932682294	0.289459564	0.274201611	1.880230442	1.909324719	0.29554275	0.319176829	BDL
0.927348497	0.135940307	0.146639338	0.962653414	0.996384288	0.15971524	0.162604748	BDL
1.50609889	0.208507732	0.217324058	1.204882277	1.325995847	0.227961066	0.206277969	BDL
1.344162723	0.171725932	0.180400182	1.118607065	1.252876214	0.171009496	0.193572509	BDL
1.367843965	0.183950013	0.205944307	1.090303134	1.142671528	0.194842941	0.174675391	BDL
1.240081991	0.156226741	0.167944576	0.966032922	1.052225333	0.166476585	0.154051837	BDL
2.049345984	0.248998902	0.26310555	1.573926802	1.492349074	0.256120207	0.280836603	BDL
0.850632282	0.129291118	0.128483722	0.852605108	0.882729399	0.158928938	0.161884927	BDL
0.840440447	0.115895892	0.122456955	0.940046714	0.901920739	0.129458827	0.145436072	BDL
1.070575313	0.161969781	0.167510713	1.164691517	1.239575181	0.201406324	0.20083174	BDL
0.102851597	0.01214772	0.012937629	0.078874415	0.082661494	0.013710249	0.012065341	BDL
-0.099025683	-0.014273405	-0.015281481	-0.079596456	-0.088985608	-0.013291563	-0.013906458	BDL
1.163195861	0.177112263	0.16524128	1.137075903	1.053820975	0.169923146	0.179387075	BDL
1.630563721	0.238337546	0.25729236	1.47921511	1.5185741	0.245154868	0.297574518	BDL
0.20038759	0.047087815	0.046807216	0.117253035	0.110832906	0.042029969	0.047533724	BDL
0.688999486	0.095028952	0.101550907	0.757926438	0.709150611	0.12582498	0.122010024	BDL
0.746189277	0.105693083	0.103375622	0.725086823	0.797587597	0.12201	0.111657982	BDL
0.832744106	0.106456402	0.111044266	0.671191237	0.59765932	0.103912802	0.099801089	BDL
1.123753442	0.158114169	0.17238145	1.107608296	0.987307736	0.156916851	0.153653022	BDL
0.708766502	0.104178706	0.160475239	0.720712547	0.741927038	0.138504349	0.171009879	BDL
0.421416399	0.05209301	0.058119487	0.293561839	0.388973423	0.042432731	0.048675395	BDL
0.659140882	0.099520816	0.094727751	0.538268508	0.516009803	0.090437047	0.095921868	BDL
1.175525161	0.142655799	0.173415702	1.200481658	1.051103672	0.198041811	0.190414154	BDL
0.417967077	0.05242774	0.060878	0.483010312	0.478999627	0.0810398	0.062633353	BDL
1.132971944	0.169798341	0.173686225	1.027066051	1.016615999	0.179359904	0.165959271	BDL
1.140566588	0.125700454	0.10880071	0.883278868	1.018000241	0.142587093	0.120478129	BDL

1.492928886	0.209730088	0.192969584	1.073916051	1.378405894	0.217167497	0.176216385	BDL
0.842833281	0.112171027	0.116231365	0.739249448	0.857943528	0.128829096	0.118480684	BDL
0.83319595	0.096276339	0.105604176	0.645246862	0.665370996	0.112226771	0.126479085	BDL
2.803828128	0.400136766	0.379750051	2.776861066	2.373832722	0.47632883	0.508587465	BDL
1.127668936	0.167587467	0.149777975	1.017629868	1.144836717	0.198374866	0.190492985	BDL
0.59885465	0.075031984	0.071235826	0.561452064	0.473407321	0.099791165	0.100222521	BDL
1.072685404	0.143518839	0.143467926	1.020462723	1.032844019	0.151187695	0.175637018	BDL
0.74057135	0.141536569	0.171968353	0.532248715	0.729636644	0.159357445	0.179024635	BDL
1.179871419	0.202701273	0.210427855	1.177804901	1.256437765	0.211287233	0.24076239	BDL
1.76833828	0.274981266	0.295612111	1.983617223	1.928039911	0.370075518	0.385367086	BDL
2.55424019	0.37216825	0.460124351	2.728248763	2.618165362	0.502641413	0.544088543	BDL
2.560641103	0.352009348	0.435724017	2.022201178	2.1637568	0.452790161	0.420467374	BDL
0.410206341	0.064685603	0.081414653	0.458309782	0.522674448	0.098307736	0.104246228	BDL
0.502363635	0.122875996	0.139206646	0.521973736	0.457298488	0.128823263	0.144107279	BDL
1.963663564	0.307935793	0.422345186	2.09801556	2.167563757	0.365371233	0.504033146	BDL
0.38970185	0.061845728	0.06318613	0.4208998	0.430759448	0.067472932	0.08555189	BDL
0.786981492	0.107365187	0.126894575	0.884926671	0.741201189	0.15004387	0.170324521	BDL
1.726033684	0.25041866	0.278554778	1.864510112	1.912270656	0.314301348	0.315154179	BDL
1.509606457	0.206403842	0.287786422	1.635708985	1.632615353	0.305863607	0.374867214	BDL
0.499069447	0.055930864	0.180708436	0.41886644	0.804717214	0.116504075	0.214255084	BDL
0.014909852	BDL	0.010117302	BDL	BDL	0.001692322	0.010097486	BDL
0.012518676	0.002158494	0.00441566	BDL	BDL	0.002820343	0.004931305	BDL
0.280850559	0.038491127	0.039241628	0.166469257	0.213617389	0.028011262	0.028409428	BDL
0.335219152	0.04149277	0.044602068	0.221762716	0.205843922	0.034541755	0.037384262	BDL

208 -> 208 Pb [He]	232 -> 232 Th [He]	238 -> 238 U [He]
9.829851963	0.302889886	0.106574818
15.20736232	0.780303387	0.274410344
4.100207393	0.781050708	0.332726085
5.059607541	0.231674617	0.083356461
36.97378505	0.295829445	0.164261217
21.17798574	3.427983232	1.785227144
9.190869096	0.569149613	0.712738035
2.138468171	0.473316443	0.246438145
4.832871597	BDL	0.128340483
9.148760342	0.092504821	0.070838322
7.900360675	2.313902028	2.368620479
12.64471552	2.464255169	0.962190853
54.05826556	1.94030042	1.214067656
5.746296649	1.446878724	0.925493975
18.37502458	4.036825485	8.580221252
1.240436647	0.401876951	0.109720765
4.417274046	1.318667289	0.612803212
7.516171405	1.257339834	0.633295653
66.42430075	7.416932196	6.540532803
5.213343214	0.853289374	0.248498536
4.406408848	0.191358381	0.130912289
37.8072686	1.358503667	1.005996886
6.62178737	0.989551294	0.589611474
12.09671523	3.436807125	1.747761549
12.0501904	2.328150211	1.97560562

23.50333173	4.984740001	3.169082005
21.197977	4.231930453	1.510989685
6.455248294	1.627568051	1.278525047
15.99753925	1.031542531	0.472504577
40.70456032	2.267783874	1.298430924
3.741174023	0.761159736	0.251833704
40.05481086	3.651073481	2.456991599
81.07750281	2.258215023	1.247712895
10.73280041	3.446558861	1.85584208
7.493602026	1.087739233	0.847021143
3.028325242	0.592847769	0.232680609
30.69799852	0.226351395	0.144741124
5.17547826	0.070275695	0.027108492
-0.656352356	BDL	-0.019538077
23.73111363	0.999919687	0.799190883
15.08914465	3.517931213	1.318483761
BDL	BDL	BDL
12.17786356	0.242379872	0.153465988
9.01793824	0.445532651	0.351751348
10.02795958	0.32475057	0.781193169
3.489332982	0.177123228	0.208711416
0.79252295	#VALUE!	0.248129115
1.667873812	0.243246584	0.392204092
0.974989447	0.495213103	1.366546834
1.176024658	BDL	0.112670245
BDL	0.246338193	0.259031164
1.722485339	0.937330829	0.663012327
BDL	BDL	1.704240166

2.956628896	2.054154623	3.724777589
3.32151174	0.500966819	1.67283482
2.751600718	BDL	1.232326905
2.303667085	BDL	3.5717666
4.431716717	0.759284451	1.460987199
1.845704967	0.312343262	2.485728913
6.361083414	0.914853716	0.957305713
0.611250119	0.390411261	0.355888813
7.852677147	2.007498179	0.955492321
5.531052005	0.799042801	1.04748086
148.1787534	3.201443838	2.634619991
BDL	BDL	1.15454327
0.748198875	1.431877674	2.835260026
4.497470646	5.70640235	8.671827001
8.643611835	2.526876352	6.455854305
7.67080056	1.515883395	1.682396973
14.51390876	0.700160996	1.240455391
3.573834257	0.155116982	0.305200416
42.80811802	4.542350785	3.950210306
26.81962529	BDL	1.212617963
BDL	BDL	0.971328219
BDL	BDL	0.718965638
BDL	BDL	0.402828095
BDL	BDL	0.513792599

Table 4: The $^{87}Sr/^{86}Sr$ data set including ICP data, raw TIMS data and the Rb in-situ decay corrected $^{87}Sr/^{86}Sr$

Sample ID	87Sr/86Sr	2se	Depth (m)	Rb (ppm)	Sr (ppm)	Measured (ICP) 87Rb/86Sr	Rb-Corrected 87Sr/86Sr(cor)	Measured (TIMS) 87Sr/86Sr
	0.72093647	0.000003	0.8	1.95370171	146.597455	0.0376	.719502	0.72093647
LS201 Sr	0.76921009	0.000475	2.4	10.6910192	54.6964997	0.5517	.748167	0.76921009
LS201 Sr rerun	0.76876906	0.000004	2.4	10.6910192	54.6964997	0.5517	.747726	0.76876906
LS202 Sr	0.72401461	0.000003	6.8	3.22832754	134.3849	0.0678	.721428	0.72401461
LS203 Sr	0.72083473	0.000003	15.8	1.30788623	309.673367	0.0119	.720380	0.72083473
LS204 Sr	.732453	.000004	22.5	1.95345762	63.309666	0.0871	.729131	.732453
LS205 Sr	.757722	.000003	24.3	27.3152881	170.284383	0.4528	.740452	.757722
LS206 Sr	0.729786	0.000003	25.65	1.6859594	146.519209	0.0325	.728547	0.729786
LS207 Sr	0.72673775	0.000003	26.3	1.73238641	98.7350664	0.0495	.724849	0.72673775
LS208 Sr	0.72694069	0.000003	27.6	1.1479766	170.996372	0.0189	.726218	0.72694069
LS 209 Sr	0.729963	0.002270	34.75	2.6205799	83.4693553	0.0886	.726583	0.729963
LS 209 Sr rerun	0.727438	0.000003	34.75	2.6205799	83.4693553	0.0886	.724058	0.727438
LS210 Sr	.740148	.000003	42.7	4.99837349	61.352528	0.2299	.731377	.740148
LS211 Sr	0.74098435	0.000003	45.4	12.0552963	148.891254	0.2285	.732267	0.74098435
LS212 Sr	.736421	.000004	46.45	10.1193246	107.341832	0.2661	.726272	.736421
LS 213 Sr	0.761912	0.000003	47.65	12.8132104	77.9178759	0.4641	.744208	0.761912
LS214 Sr	.756021	.000004	48.85	9.03247805	54.8846508	0.4645	.738303	.756021
LS215 Sr	0.73018469	0.000003	49.9	11.6692069	209.412251	0.1573	.724185	0.73018469
LS216 Sr	0.72745043	0.000003	51.55	4.73118824	307.456569	0.0434	.725794	0.72745043
LS217 Sr	0.75557123	0.000003	54.1	26.6587059	152.3382	0.4939	.736731	0.75557123
LS 218 Sr	0.830082	0.000006	56.3	18.9433614	29.8048327	1.7939	.761655	0.830082

LS219 Sr	0.733524	0.000003	58.2	9.62386518	190.608905	0.1425	.728088	0.733524
LS220 Sr	0.73815153	0.000003	58.9	12.7651586	308.456569	0.1168	.733696	0.73815153
LS 221 Sr	0.733088	0.000003	60.8	15.375991	313.646877	0.1384	.727810	0.733088
LS 222 Sr	0.741911	0.000003	63.2	7.05866999	88.6916366	0.2246	.733343	0.741911
LS 223 Sr	0.776736	0.000004	64.3	19.5651593	78.5927514	0.7026	.749935	0.776736
LS224 Sr	.778172	.000002	66.05	22.0912047	96.9604625	0.6431	.753643	.778172
LS225 Sr	1.061239	.000006	69.45	90.1346266	58.2834385	4.3650	.894743	1.061239
LS 226 Sr	0.863562	0.000004	71.4	35.4084256	57.4657563	1.7391	.797225	0.863562
LS227 Sr	0.764655	0.000004	77.5	25.6419663	177.665897	0.4074	.749117	0.764655
LS228 Sr	.753034	.000004	82.9	13.2201296	119.821611	0.3114	.741156	.753034
LS229 Sr	.820165	.000004	86.5	47.9020454	116.717725	1.1584	.775980	.820165
LS230 Sr	.758647	.000003	88.4	13.5949588	93.5686701	0.4101	.743005	.758647
LS231 Sr	0.97719169	0.000007	90.5	61.1752829	57.2145755	3.0179	.862078	0.97719169
LS231 Sr	0.977192	0.000007	90.5	61.1752829	57.2145755	3.0179	.862078	0.977192
LS 232 Sr	0.826189	0.000005	91.2	21.6226504	58.8140038	1.0377	.786608	0.826189
LS233 Sr	.799882	.000003	93	151.050337	75.606851	5.6389	.584793	.799882
LS 234 Sr	0.762495	0.000003	96.6	16.3520329	89.829629	0.5138	.742898	0.762495
LS235 Sr	.767845	.000003	99.1	39.1687612	152.804626	0.7235	.740248	.767845
LS236 Sr	.753333	.000003	100	20.2025761	142.984469	0.3988	.738121	.753333
LS237 Sr	0.759090	0.000176	101.95	4.72481111	22.7738987	0.5856	.736754	0.759090
LS237 Sr rerun	0.759855	0.000004	101.95	4.72481111	22.7738987	0.5856	.737519	0.759855
LS238 Sr	.759183	.000003	105.1	-3.83845228	-17.0309786	0.6361	.734919	.759183
LS 239 Sr	0.783940	0.000020	107.1	66.1755105	173.582692	1.0760	.742896	0.783940
LS 239 Sr rerun	0.783936	0.000004	107.1	66.1755105	173.582692	1.0760	.742892	0.783936
LS240 Sr	.795477	.000003	109.4	63.0566636	207.686105	0.8570	.762789	.795477
LS 241 Sr	0.746267	0.000003	117.6	8.45334876	54.5495745	0.4374	.729583	0.746267
LS242 Sr	.729357	.000005	121.3	2.27208809	147.546992	0.0435	.727699	.729357

LS 243 Sr	0.775037	0.000003	123.5	32.0347226	97.5869748	0.9265	.739696	0.775037
LS244 Sr	0.75395592	0.000005	126.4	20.8102047	136.065874	0.4317	.737490	0.75395592
LS 245 Sr	0.755753	0.000014	129.95	32.3582573	139.313771	0.6556	.730747	0.755753
LS 245 Sr	0.755704	0.000004	129.95	32.3582573	139.313771	0.6556	.730698	0.755704
LS246 Sr	1.166640	.000008	133	42.0253826	92.3811088	1.2840	1.117664	1.166640
LS247 Sr	.790394	.000003	138.1	52.2864751	122.83269	1.2015	.744566	.790394
LS 248 Sr	0.759431	0.000004	138.7	34.3063285	156.204684	0.6199	.735786	0.759431
LS249 Sr	0.760239	0.000004	146.7	41.9699234	173.86651	0.6813	.734251	0.760239
LS 250 Sr	0.727994	0.000004	495	3.68025588	277.821329	0.0374	.726567	0.727994
LS251 Sr	0.732439	0.000003	498.8	10.4432737	179.980849	0.1638	.726192	0.732439
LS255 Sr	.740603	.000004	513	16.0138167	152.379825	0.2966	.729289	.740603
LS257 Sr	.741430	.000004	520	11.2091396	116.69399	0.2711	.731088	.741430
LS260 Sr	.736009	.000003	531	3.95410167	134.309827	0.0831	.732839	.736009
LS261 Sr	0.733823	0.000002	534.2	6.4759011	131.886853	0.1386	.728537	0.733823
LS 262 Sr	0.736113	0.000020	537.2	31.2921602	584.421297	0.1511	.730349	0.736113
LS 262 Sr	0.736159	0.000002	537.2	31.2921602	584.421297	0.1511	.730395	0.736159
LS 263 Sr	0.727662	0.000145	540.2	8.36739822	167.319046	0.1412	.722278	0.727662
LS264 Sr	.727324	.000144	544.4	1.85554468	91.084218	0.0575	.725131	.727324
LS264 Sr	.727305	.000116	544.4	1.85554468	91.084218	0.0575	.725112	.727305
LS265 Sr	.728481	.000003	546.2	3.28348586	94.739104	0.0978	.724750	.728481
LS266 Sr rerun	.733552	.000003	548.3	1.8314158	22.0711941	0.2342	.724618	.733552
LS268 Sr	.745693	.000003	551.8	6.30530316	57.3312503	0.3104	.733852	.745693
LS270 Sr rerun	.734260	.000004	553.9	3.38629531	74.2554287	0.1287	.729350	.734260
LS272 Sr	.810606	.000005	555.2	49.2484247	127.270372	1.0922	.768945	.810606
LS274 Sr	.839010	.000004	557.15	29.5043312	54.0341538	1.5412	.780224	.839010
LS276 Sr	0.734334	0.000003	559.2	0.82905501	46.1574324	0.0507	.732401	0.734334
LS278 Sr	0.79561219	0.000006	564.25	7.31102216	18.1093776	1.1395	.752148	0.79561219
LS280 Sr	0.95862987	0.000005	569	123.139802	60.2217134	5.7714	.738488	0.95862987

LS282 Sr	.738788	.000003	573	3.49447827	32.0888553	0.3074	.727064	.738788
LS285 Sr rerun	.727507	.000003	581.05	4.88815485	165.656331	0.0833	.724330	.727507
LS290 Sr	.744322	.000003	591.35	9.52744769	68.3259609	0.3936	.729309	.744322
LS295 Sr	0.803133	0.000004	604	37.2282507	89.4807257	1.1743	.758341	0.803133
LS 300 Sr	0.816827	0.000003	622.3	29.5684659	38.8224874	2.1497	.734829	0.816827

Table 5. The colour representation of the IRMS data set presented below

Tumbiana Formation	
Hardey Formation	
First Run Carbon	
Second Run Carbon	
Third Run Carbon	

Table 6: The IRMS $\delta^{13}C$ data set. The samples too low in carbonate are not listed and the best recorded data point is indicated by its run colour.

Final Data δ13C	Depth (m)	Sample ID
-8.87	0.8	200
-8.42	2.4	201
-7.97	6.8	202
-10.94	15.8	203
-9.21	22.5	204
	24.3	205
-5.64	25.65	206
-6.83	26.3	207
-12.00	27.6	208
-16.32	34.75	209
-8.96	42.7	210
-7.77	45.4	211
-6.40	46.45	212
	47.65	213
-6.0225	48.85	214
-6.555	49.9	215
-4.7925	51.55	216
-6.42	54.1	217
-4.72	56.3	218
-6.06	58.2	219

-6.68	58.9	220
-4.78	60.8	221
-3.21	63.2	222
-5.80	64.3	223
-5.07	66.05	224
	69.45	225
-5.01	71.4	226
-5.71	77.5	227
-4.81	82.9	228
-6.31	86.5	229
	88.4	230
	90.5	231
-4.42	91.2	232
	93	233
-4.36	96.6	234
-4.13	99.1	235
-4.55	100	236
-5.53	101.95	237
-5.36	105.1	238
-6.00	107.1	239
-5.72	109.4	240
-7.31	117.6	241
-3.08	121.3	242
-3.32	123.5	243
-3.10	126.4	244
-4.03	129.95	245
-3.57	133	246
-3.20	138.1	247

-3.45	138.7	248
-3.37	146.7	249
-6.14	495	250
-7.54	498.8	251
-7.37	502.8	252
-7.72	507	253
-8.69	509.8	254
	513	255
-6.89	517.8	256
-6.80	520	257
-8.16667	523	258
-6.285	526.8	259
-10.96	530.8	260
-11.3475	534	261
-10.075	537	262
-11.5275	540	263
-10.74	544.2	264
-8.635	546	265
-4.58	548.1	266
-3.04	550.75	267
	551.6	268
-3.53	552.65	269
-3.44	553.7	270
	554.7	271
-5.52	555	272

-2.43	556	273
	557.05	274
	557.8	275
-2.81	559	276
-4.75	561.8	277
	564.05	278
-7.92	568	279
	568.8	280
-4.30	571.8	281
-6.82	572.7	282
-4.05	574.9	283
-6.89	576.8	284
-7.64	579.85	285
-8.27	583	286
	584	287
-4.66	586	288
	586.8	289
-5.58	591.15	290
-5.36	595	291
-3.68	597.5	292
-7.10	598.8	293
-7.48	600.1	294
-3.70	603.8	295
-4.97	608.8	296
-5.69	612.1	297
	615.7	298
	618.7	299
	622.1	300

	626.3	301
	629	302
-4.4575	633	303
	636	304
	639.4	305
	641.3	306
	642.5	307
	643.9	308